

Encoding and decoding of voluntary movement control in the motor cortex

Martin Nawrot

Oct 12, 2011

Introduction

Introduction

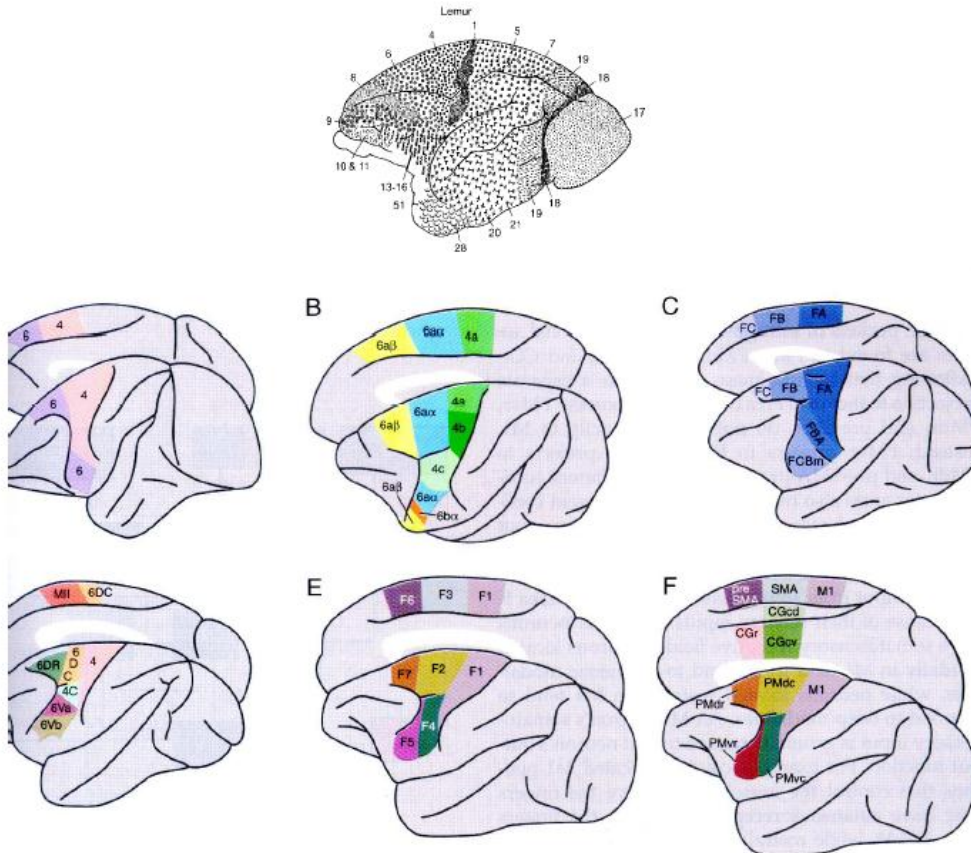


FIGURE 33.2 Cortical motor areas. Diagrams of a macaque brain show how the motor cortex of the frontal lobe has been parceled in various cytoarchitectonic studies over the past century. Modified from Matelli *et al.* (A) Brodmann, 1903; (B) Vogt and Vogt, 1919; (C) Von Bonin and Bailey, 1947; (D) Barbas and Pandya, 1987; (E) Mattelli *et al.*, 1991; (F) general abbreviations.

Cortical areas are defined as motor, if

1. they project to other motor structure
2. their ablation causes deficits in movement
3. their stimulation causes movement

Separation and further subdivision by means of

1. cytoarchitectonics
2. myeloarchitectonics
3. neurotransmitter receptor ditribution

Introduction

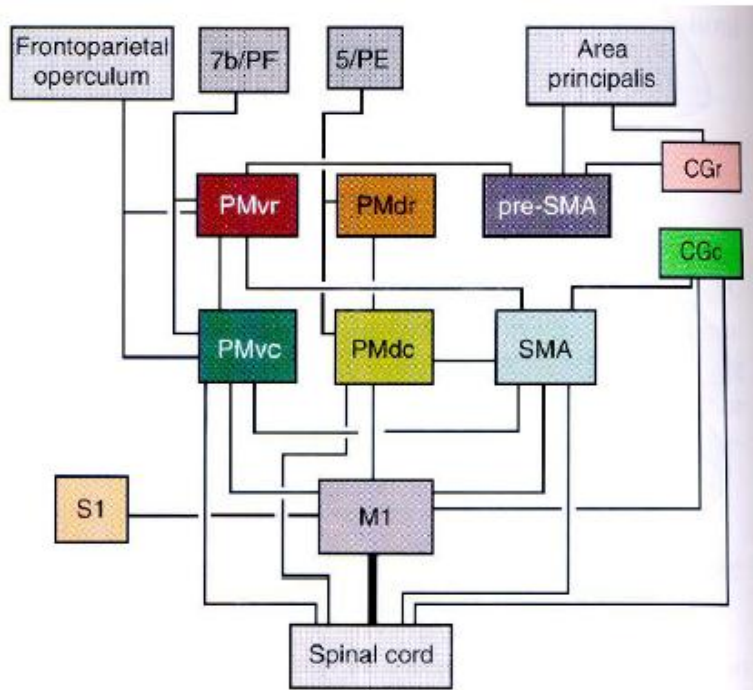
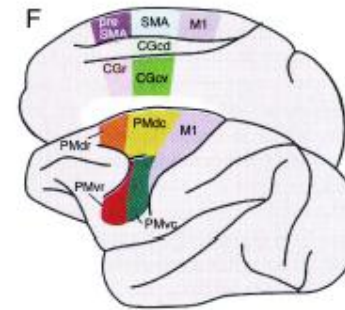


FIGURE 33.3 Connections of the cortical motor areas. Most corticocortical connections are reciprocal. Thin lines to the spinal cord from PMvc, PMdc, SMA, and CGc indicate that corticospinal projections from these areas are not as strong as that from M1.

- M1 neurons have somatosensory receptive fields (possibly via S1) related to that neuron's output function
- S1→M1 may be involved in long loop responses
- PMv neurons have large somatosensory and visual receptive fields which are related



Generic description	Generic abbreviation
Primary motor cortex	M1
Premotor cortex, dorsal caudal	PMdc
Supplementary motor area-proper	SMA
Premotor cortex, ventral, caudal	PMvc
Premotor cortex, ventral, rostral	PMvr
Pre-SMA	Pre-SMA
Premotor cortex, dorsal, rostral	PMdr
Cingulate motor area, caudal	CGc
Cingulate motor area, rostral	CGr

Introduction

cytoarchitectonics of motor cortical layers IV and V

- Area 4
 - giant pyramidal cells of Betz in layer V
 - almost no layer IV neurons (agranular cortex)
- Area 6
 - smaller layer V neurons
 - few layer IV neurons (dysgranular cortex)
- Only fibres from layer V leave cortex as a system (i.e., other efferents connect to intracortical targets)

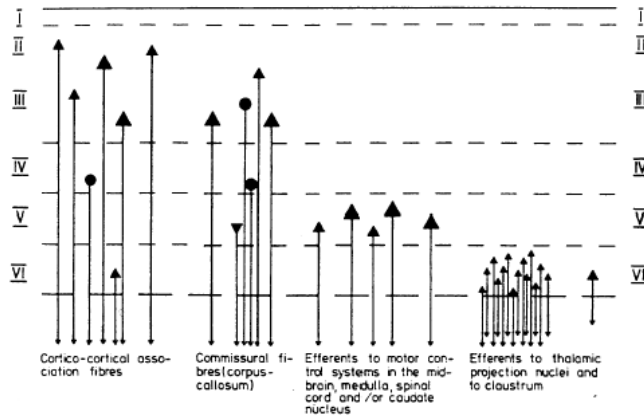
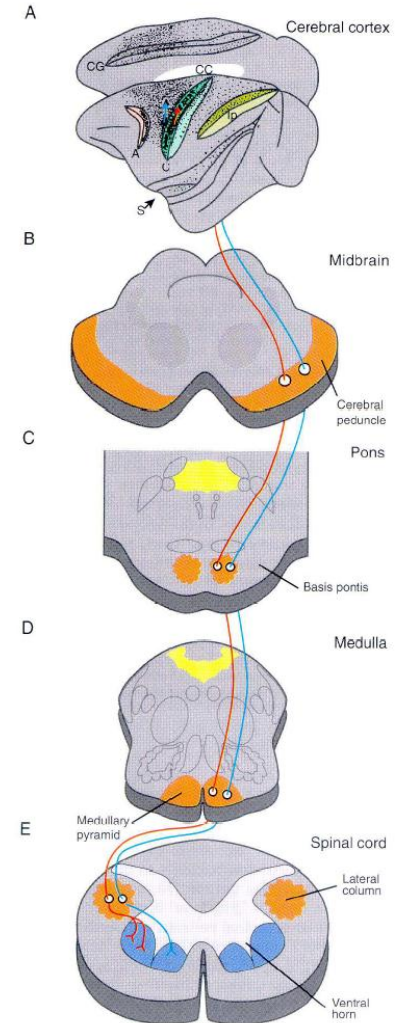
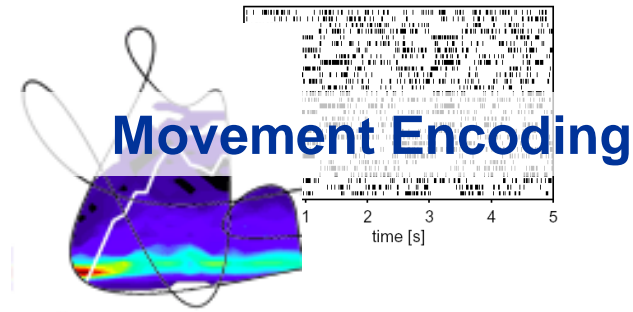


Fig. 3-35: Schematic representation of the laminar organization of the cortical efferents. The localization of the neuron bodies is shown. The predominant recipient lamina of the cortex is Lamina IV in which the afferent thalamocortical fibers terminate. The apical dendrites extending through lamina IV from the efferent lamina V (and lamina VI) as well as the basal dendrites of lamina III pyramidal cells receive excitatory inputs from the thalamocortical terminals in lamina IV as well as excitatory and inhibitory inputs from stellate cells (cf. Fig. 3-25).

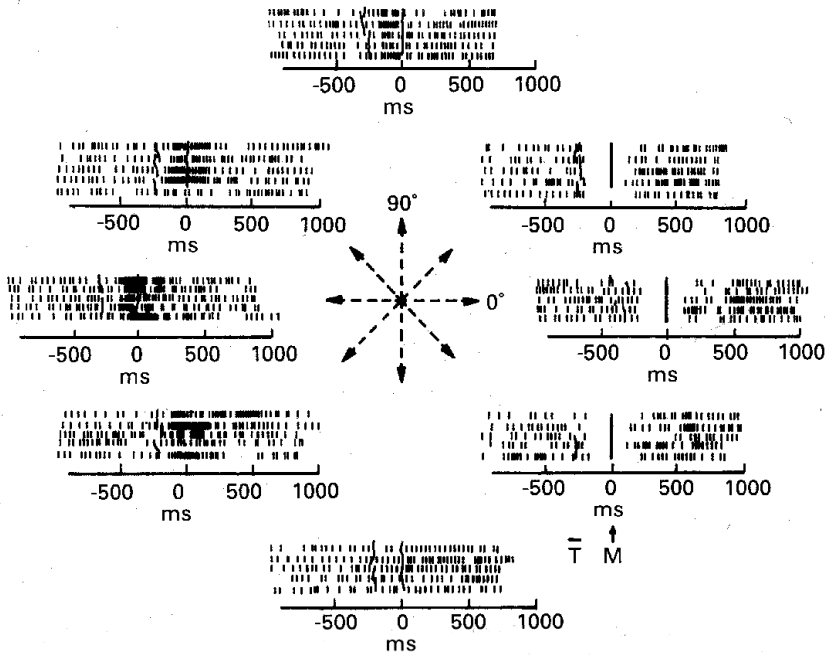
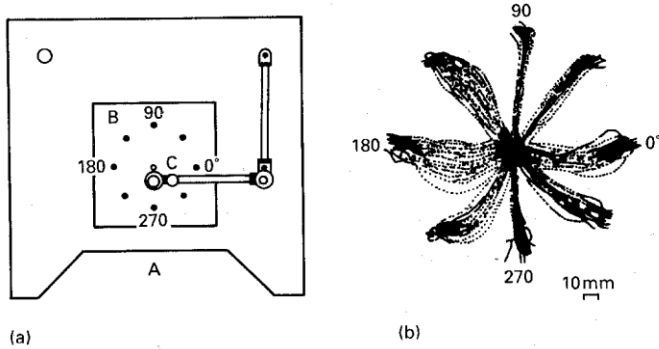
cortico-spinal tract



Encoding of Movement Parameters in the Motor Cortex



Directional tuning of motor cortical cells



Georgopoulos et al. (1982) *J. Neuroscience*

Directional tuning of motor cortical cells

EXERCISE 1 : Estimate Tuning Curve

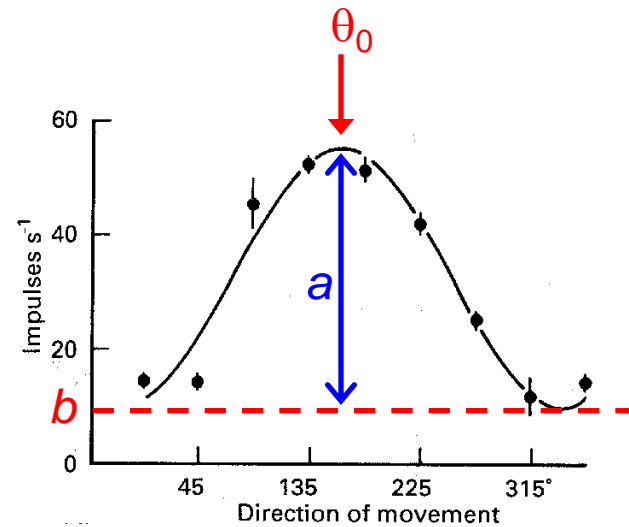
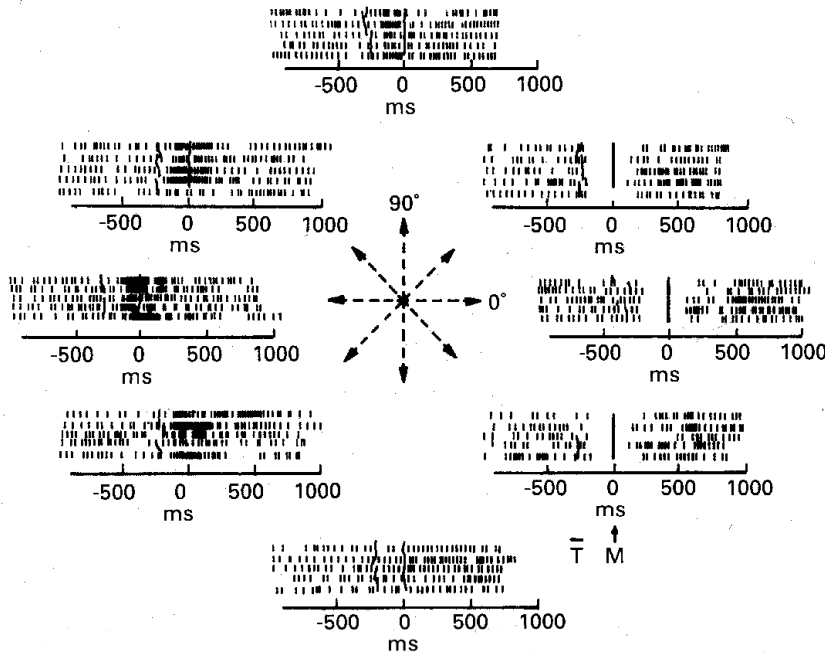
Cosine tuning:

$$f = b + a \cos(\theta_i - \theta_0)$$

θ_i : movement direction

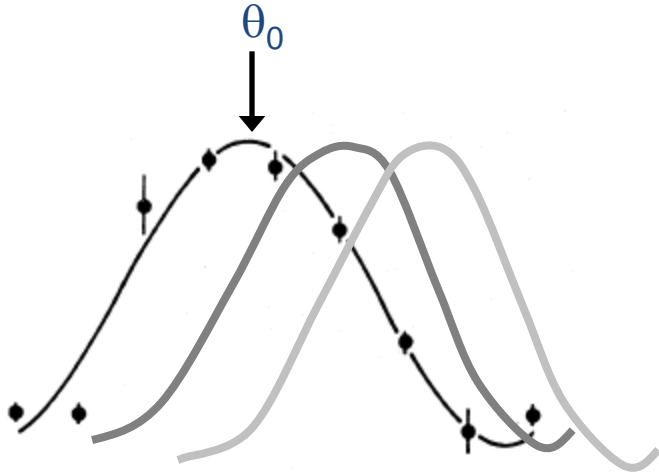
f : discharge rate

θ_0 : preferred direction



Georgopoulos et al. (1982) *J. Neuroscience*

Directional tuning of motor cortical cells

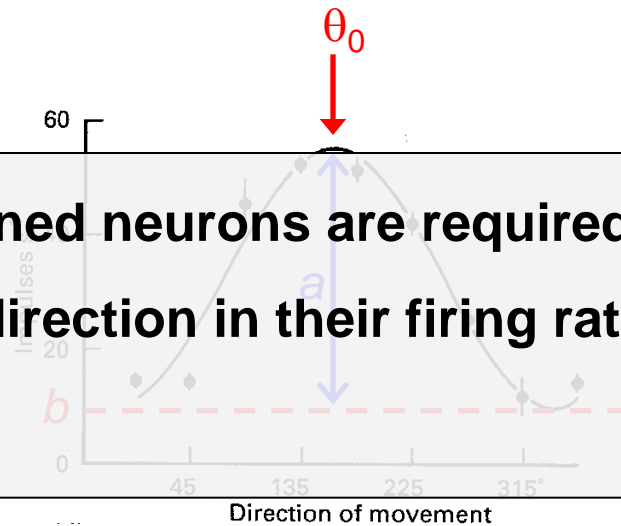


Cosine tuning:

$$f_i = b + a \cos (\theta_i - \theta_0)$$

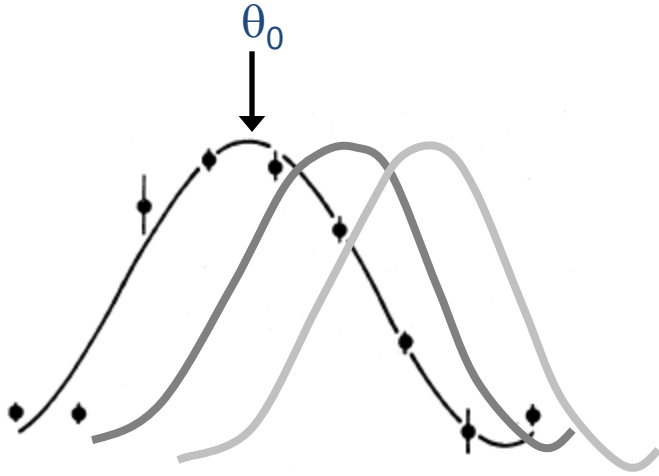
i : movement direction
 f : discharge rate
 θ_0 : preferred direction

- **How many independently cosine tuned neurons are required to unambiguously encode movement direction in their firing rate (noise-free case)?**

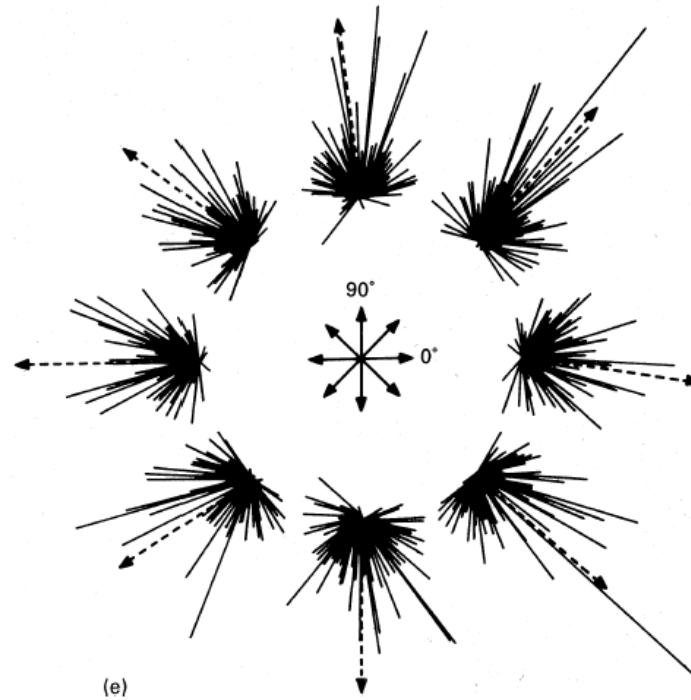


Georgopoulos et al. (1982) *J. Neuroscience*

Directional tuning of motor cortical cells



individual cells show
broad tuning with
individual preferred direction
(*assumption: cells are independent*)



population vector:

$$\vec{P} = \sum (f_i - b_i) \vec{p}_i$$

Georgopoulos et al. (1982) J. Neuroscience

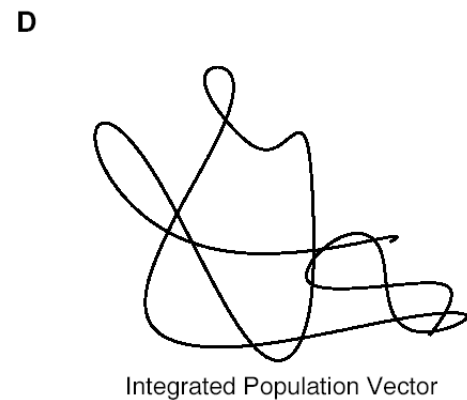
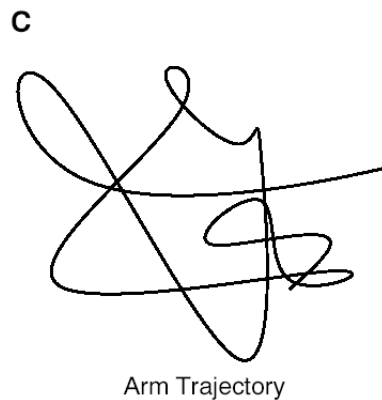
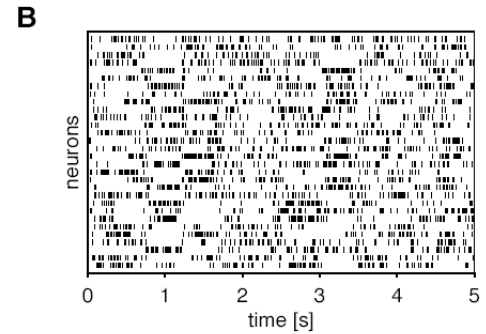
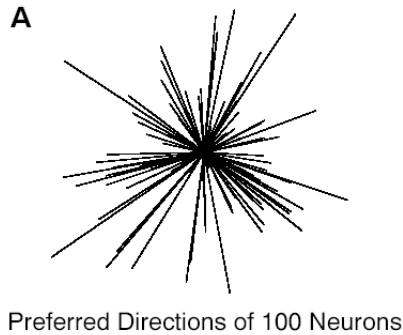
Decoding direction and speed with population vector

Directional tuning:

$$f_i(t) = g_i + \vec{p}_i \cdot \vec{v}(t)$$

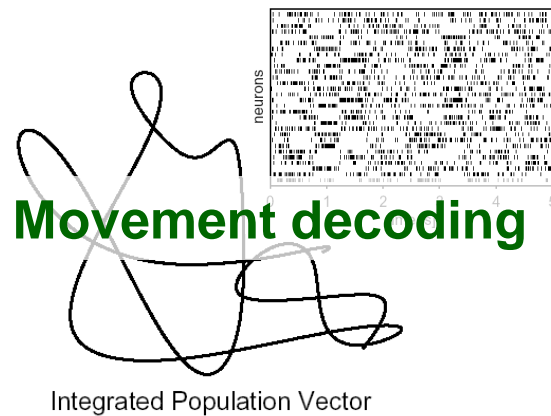
Population vector:

$$\vec{v}(t) = \sum_i [f_i(t) - g_i] \vec{p}_i$$



Nawrot, Aertsen, Rotter (1999) *J. Neurosci. Meth* 94.

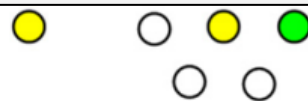
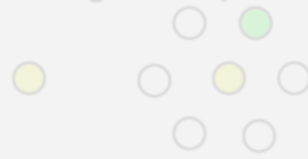
Bayesian Movement Decoding



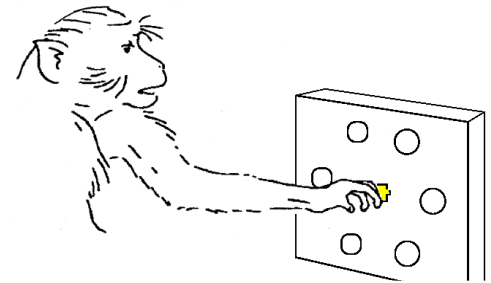
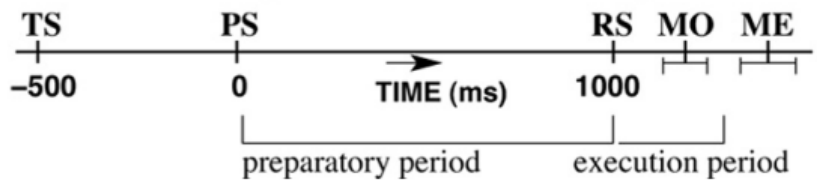
Experimental Task : Preparatory Paradigm

Data for EXERCISES 1 + 2

A 1 Target / complete Information

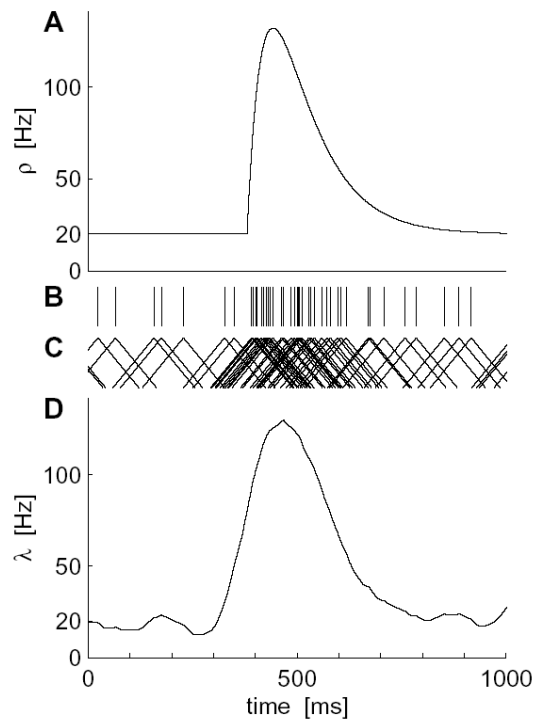
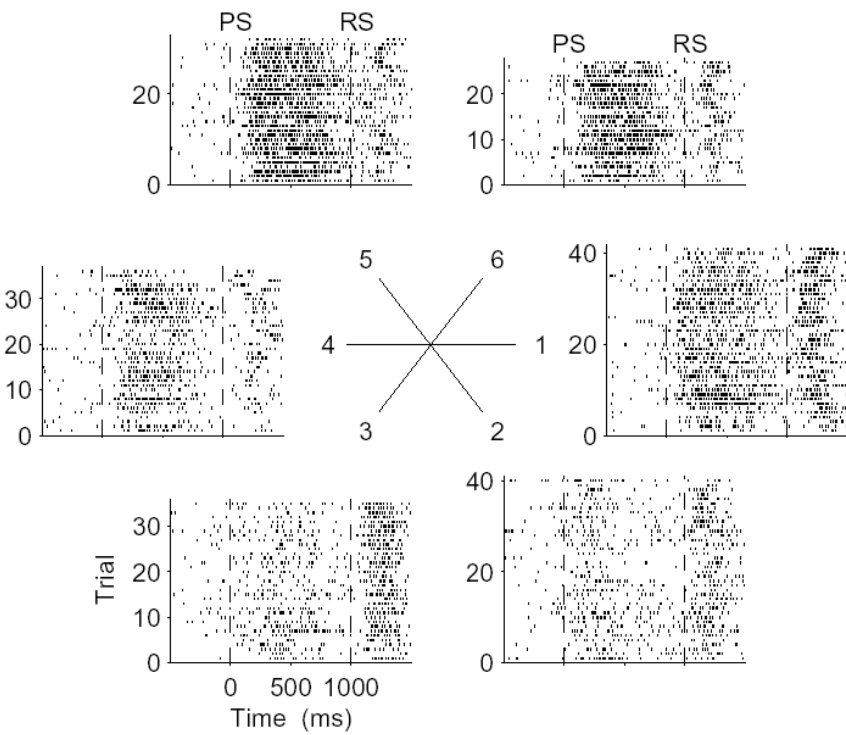


B



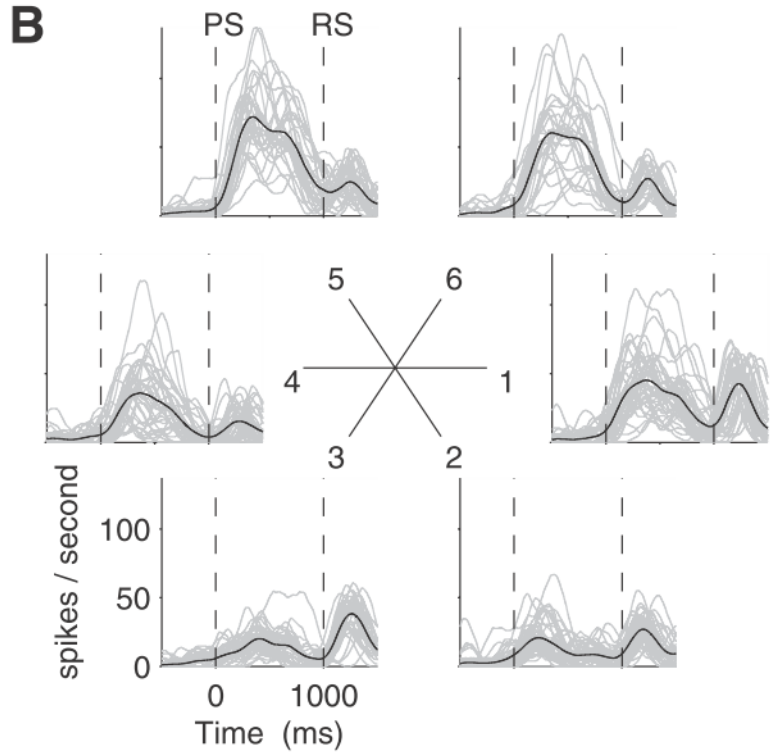
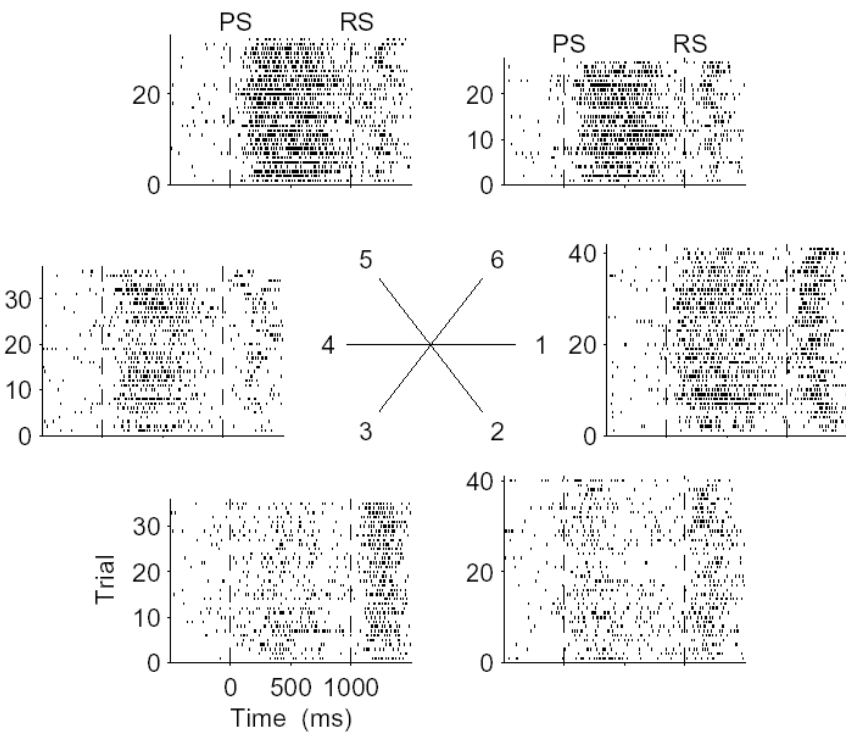
Rickert, Riehle, Aertsen, Rotter, Nawrot (2009) J Neuroscience 29

Time-resolved directional tuning



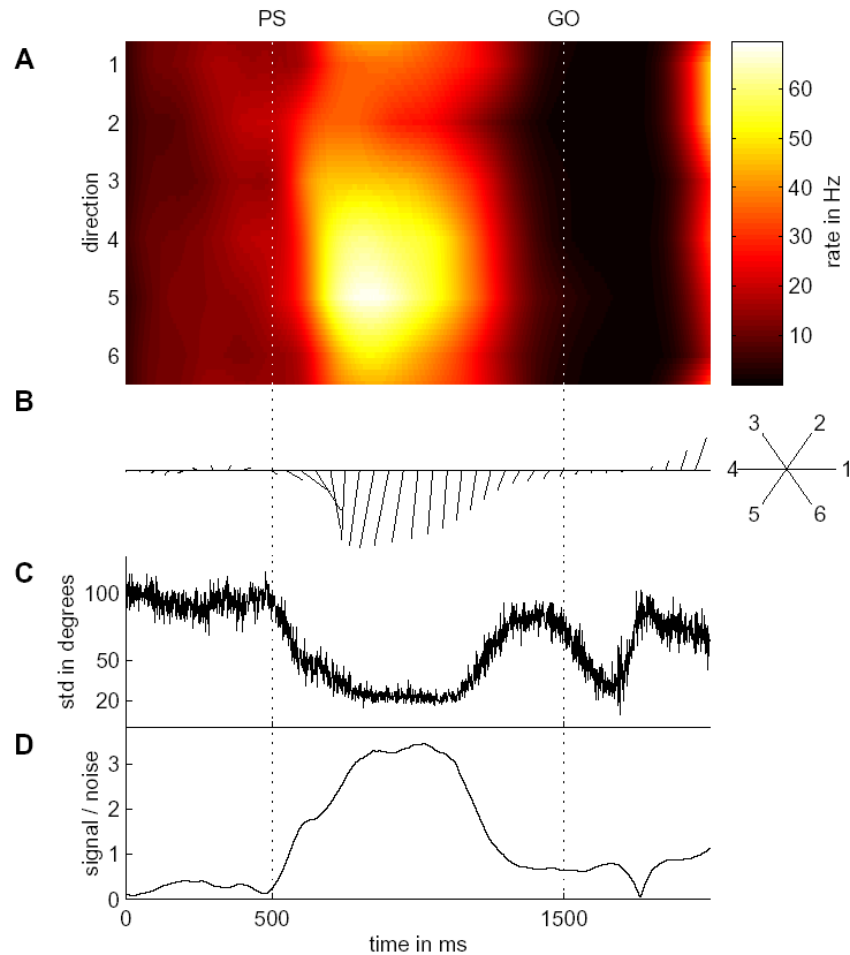
Rickert, Riehle, Aertsen, Rotter, Nawrot (2009) *J Neuroscience* 29

Time-resolved directional tuning



Rickert, Riehle, Aertsen, Rotter, Nawrot (2009) *J Neuroscience* 29

Time-resolved directional tuning



◀ Time-resolved Tuning Profile

◀ Tuning Vector

◀ Angular Deviation

◀ Signal-to-Noise Ratio

Rickert, Riehle, Aertsen, Rotter, Nawrot (2009) J Neuroscience 29

Bayesian Decoding (Naïve Bayes Classifier)

Question:

Is it possible to predict the animal's behavior (e.g. direction of the upcoming movement) from neuronal activity (e.g. instantaneous firing rate) in the single trial, despite the high variability?

Information used by an 'ideal observer':

d = movement direction

r = firing rate

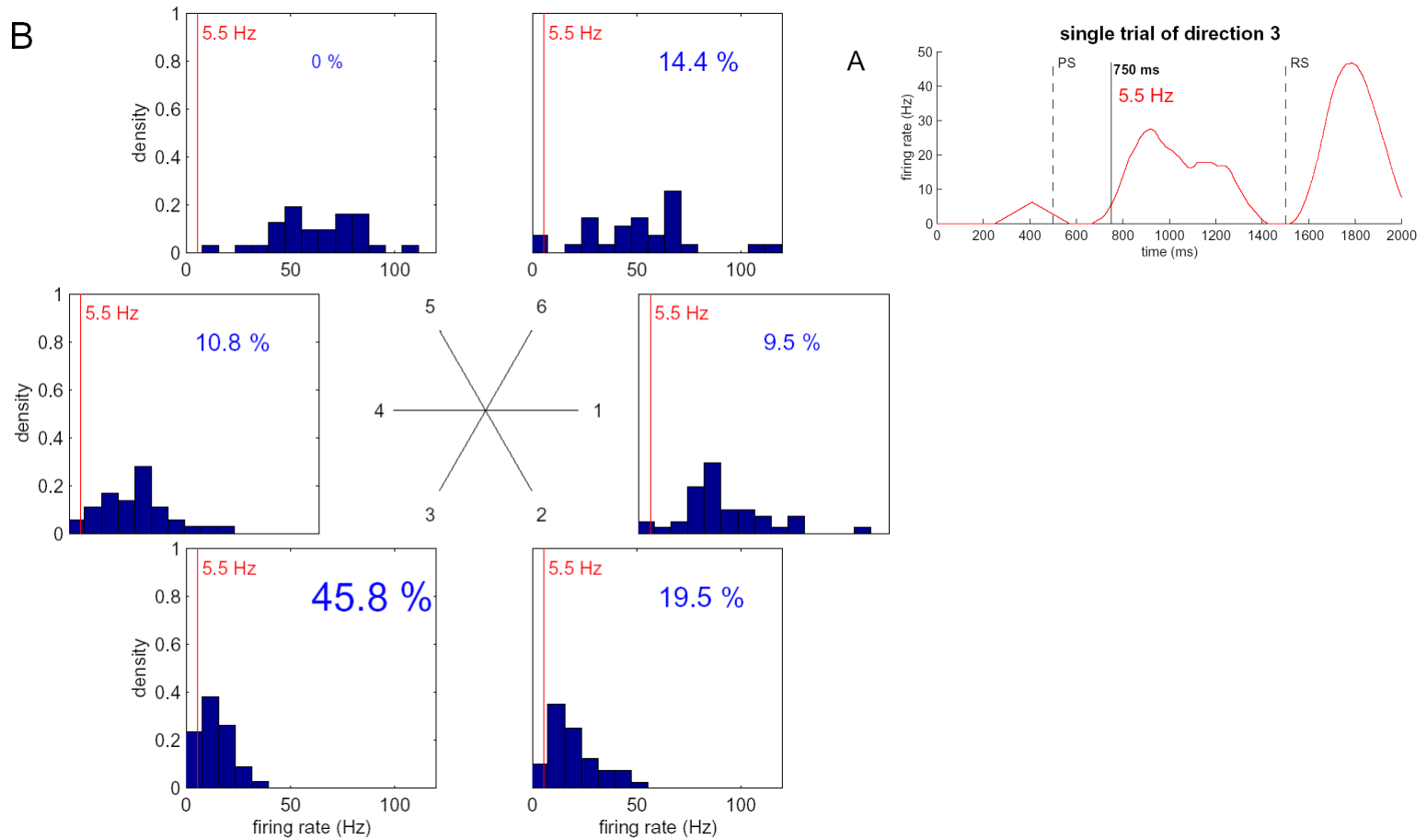
$P(r | d)$ = directional tuning profile

$P(d | r)$ = 'prediction' of direction from rate

Bayes' Rule:

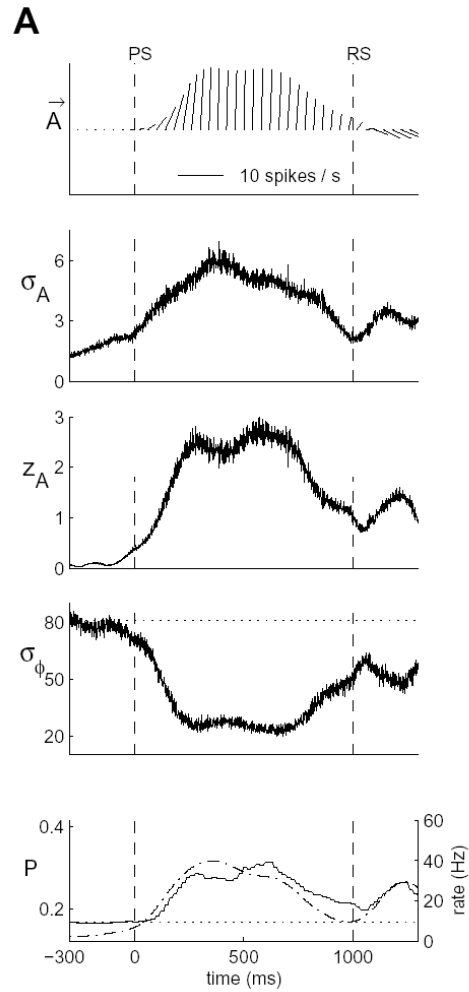
$$P(d | r) = P(r | d) \cdot \frac{P(d)}{P(r)}$$

Bayesian Decoding : Firing rate distributions



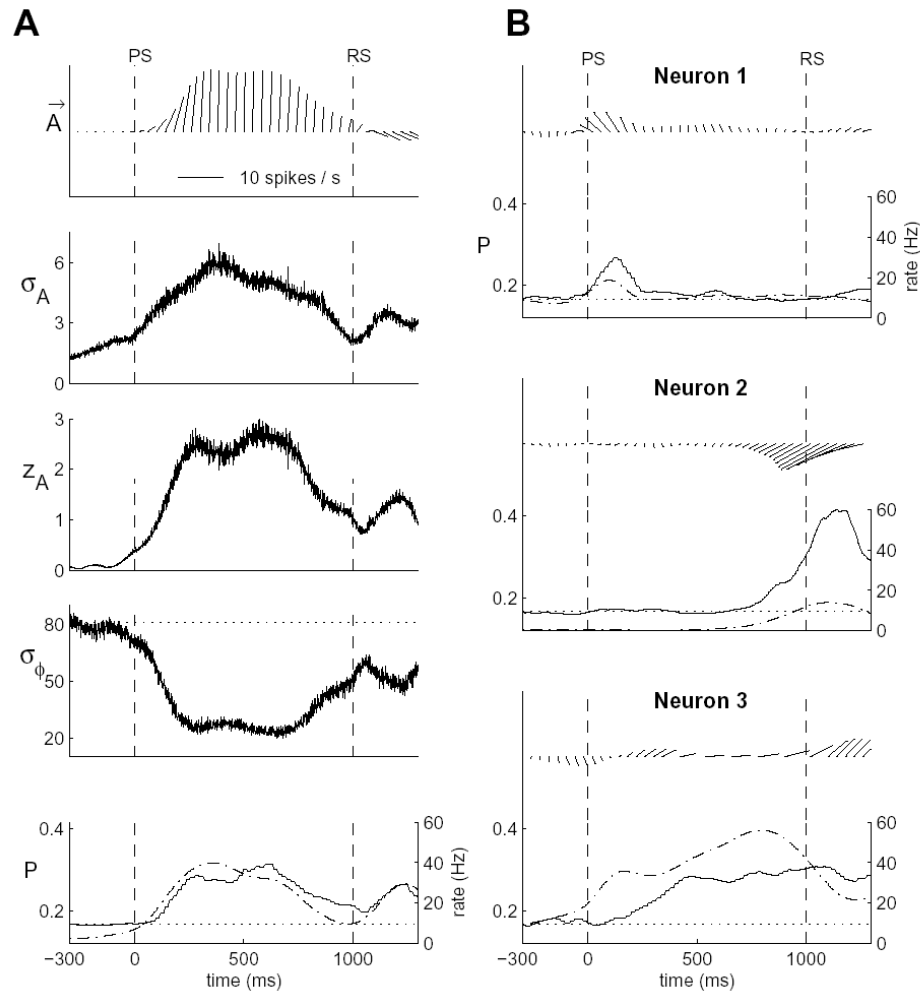
Rickert, Riehle, Aertsen, Rotter, Nawrot (2009) J Neuroscience 29

Time-resolved decoding from single neurons



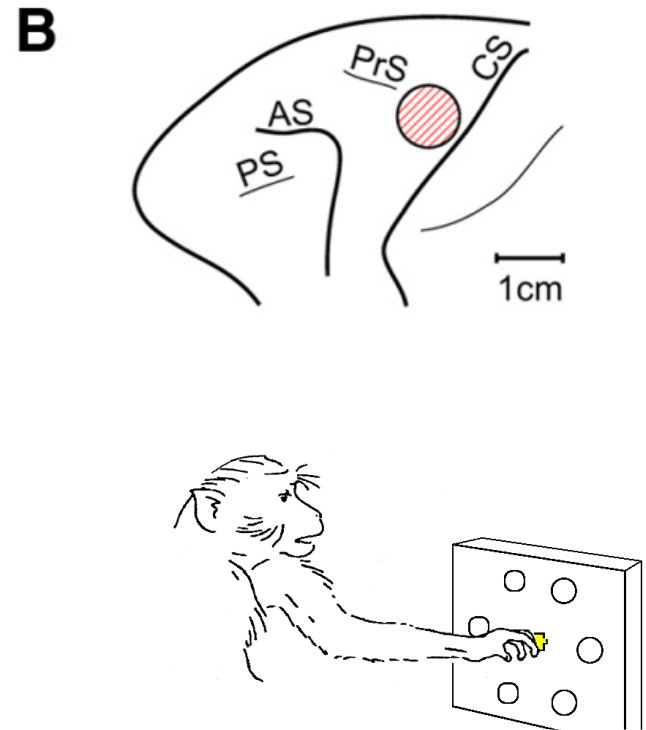
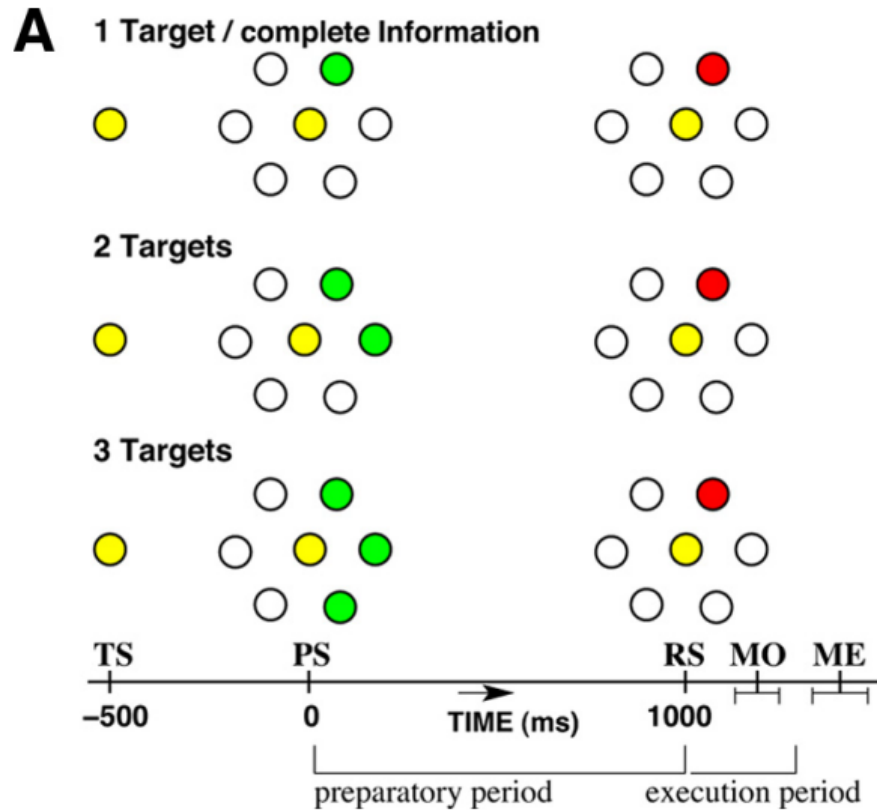
Rickert, Riehle, Aertsen, Rotter, Nawrot (2009) J Neuroscience 29

Time-resolved decoding from single neurons



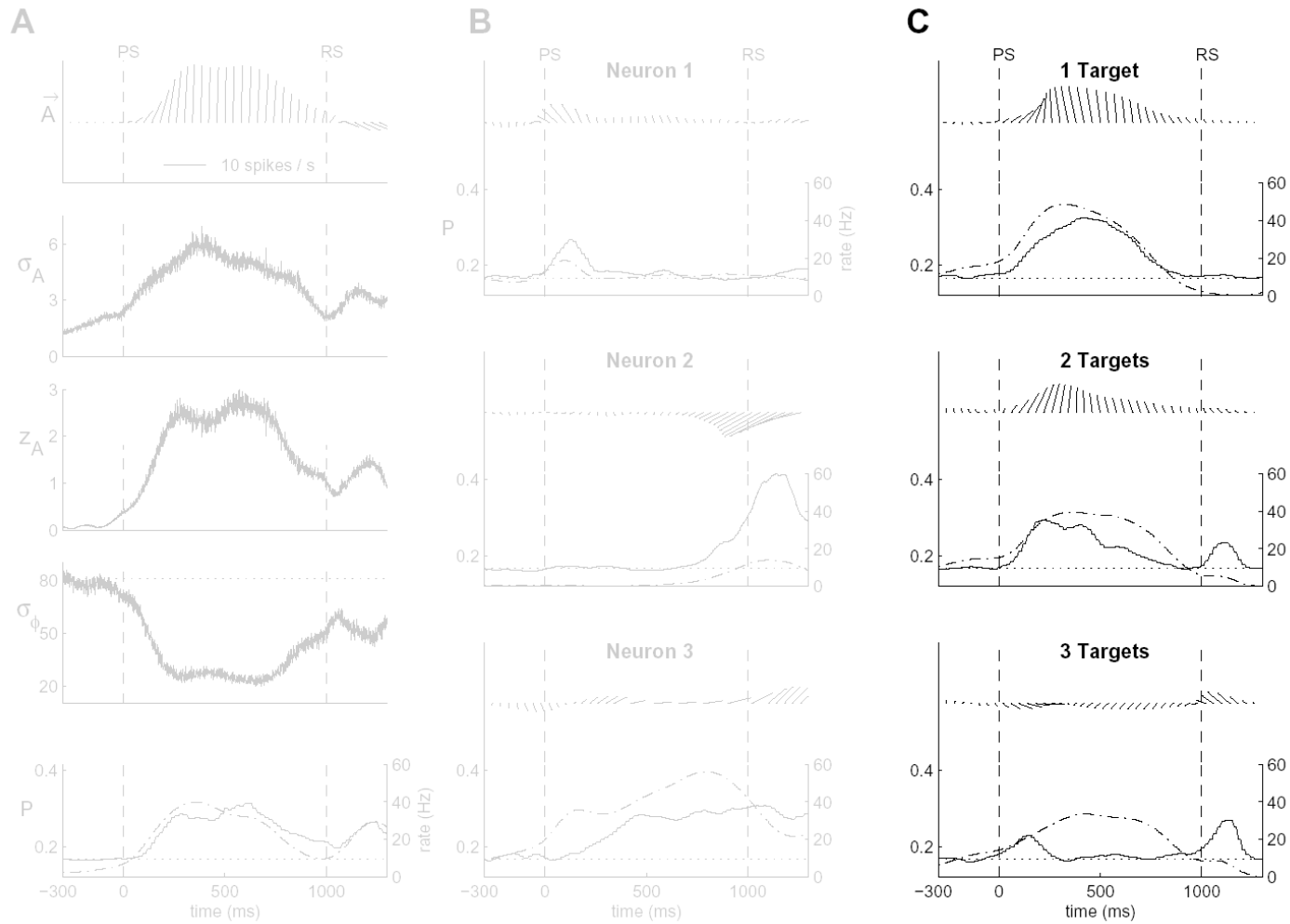
Rickert, Riehle, Aertsen, Rotter, Nawrot (2009) *J Neuroscience* 29

Time-resolved decoding from single neurons



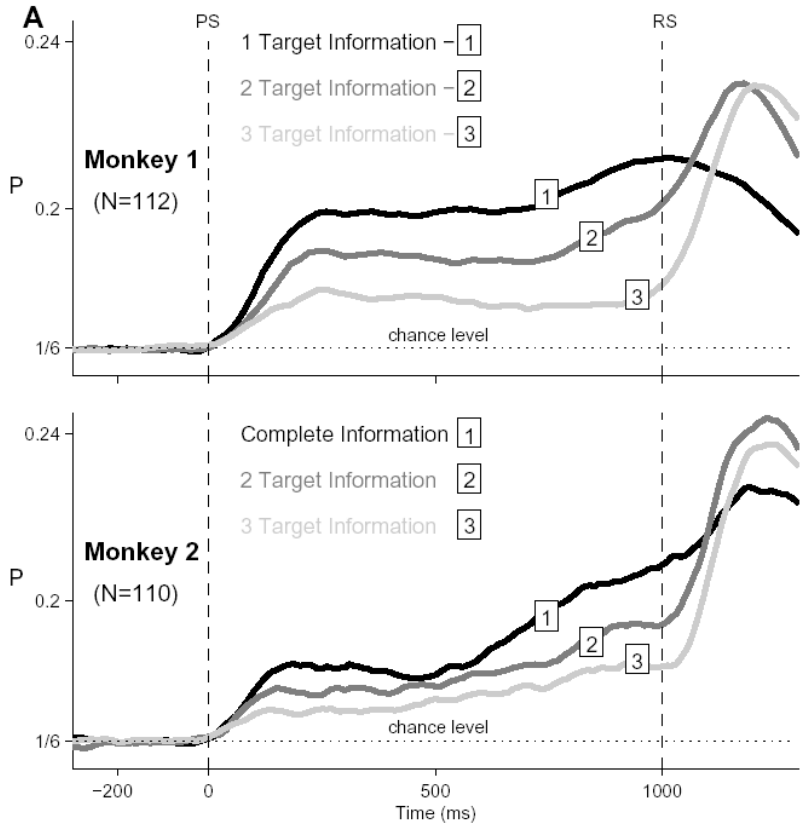
Rickert, Riehle, Aertsen, Rotter, Nawrot (2009) J Neuroscience 29

Time-resolved decoding from single neurons



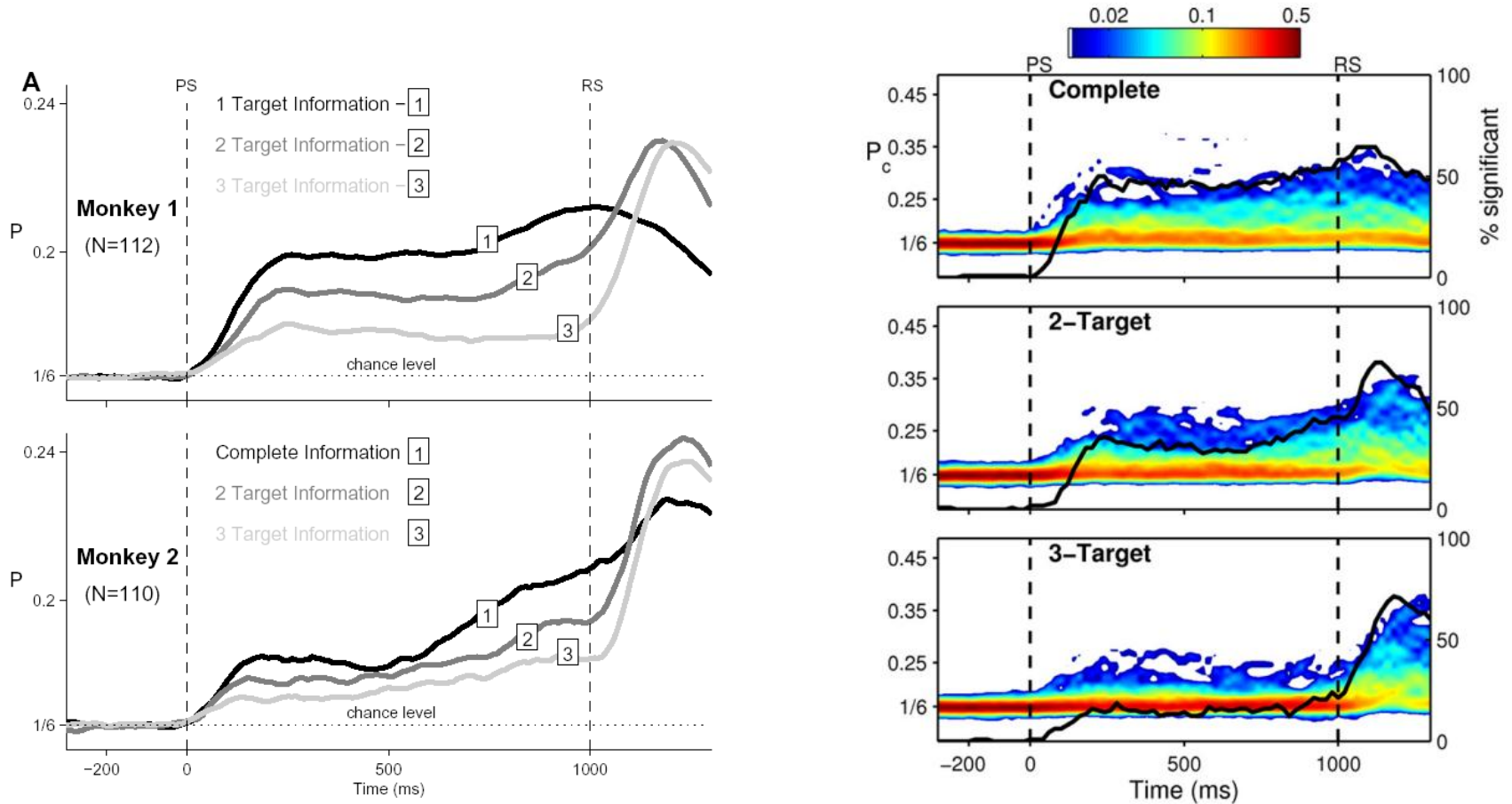
Rickert, Riehle, Aertsen, Rotter, Nawrot (2009) *J Neuroscience* 29

Time-resolved decoding from single neurons



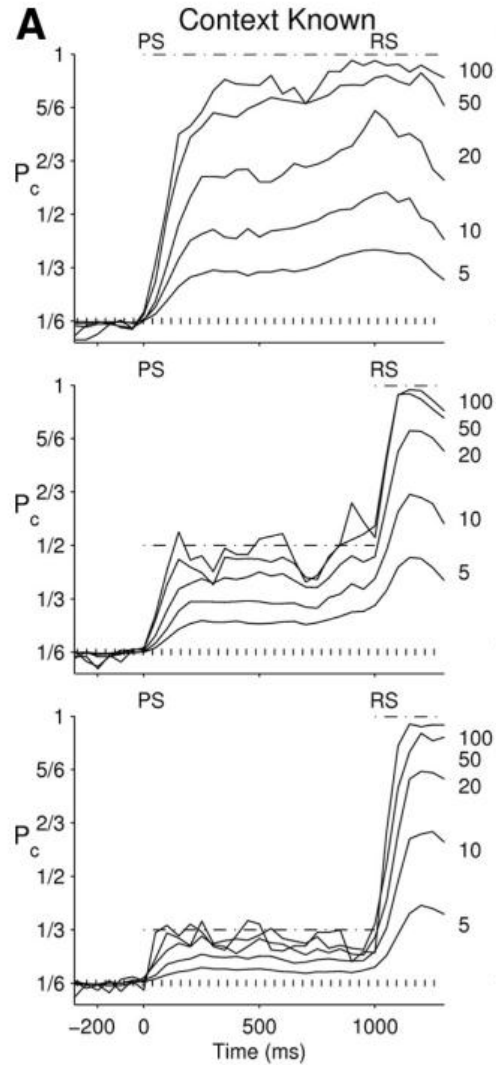
Rickert, Riehle, Aertsen, Rotter, Nawrot (2009) *J Neuroscience* 29

Time-resolved decoding from single neurons



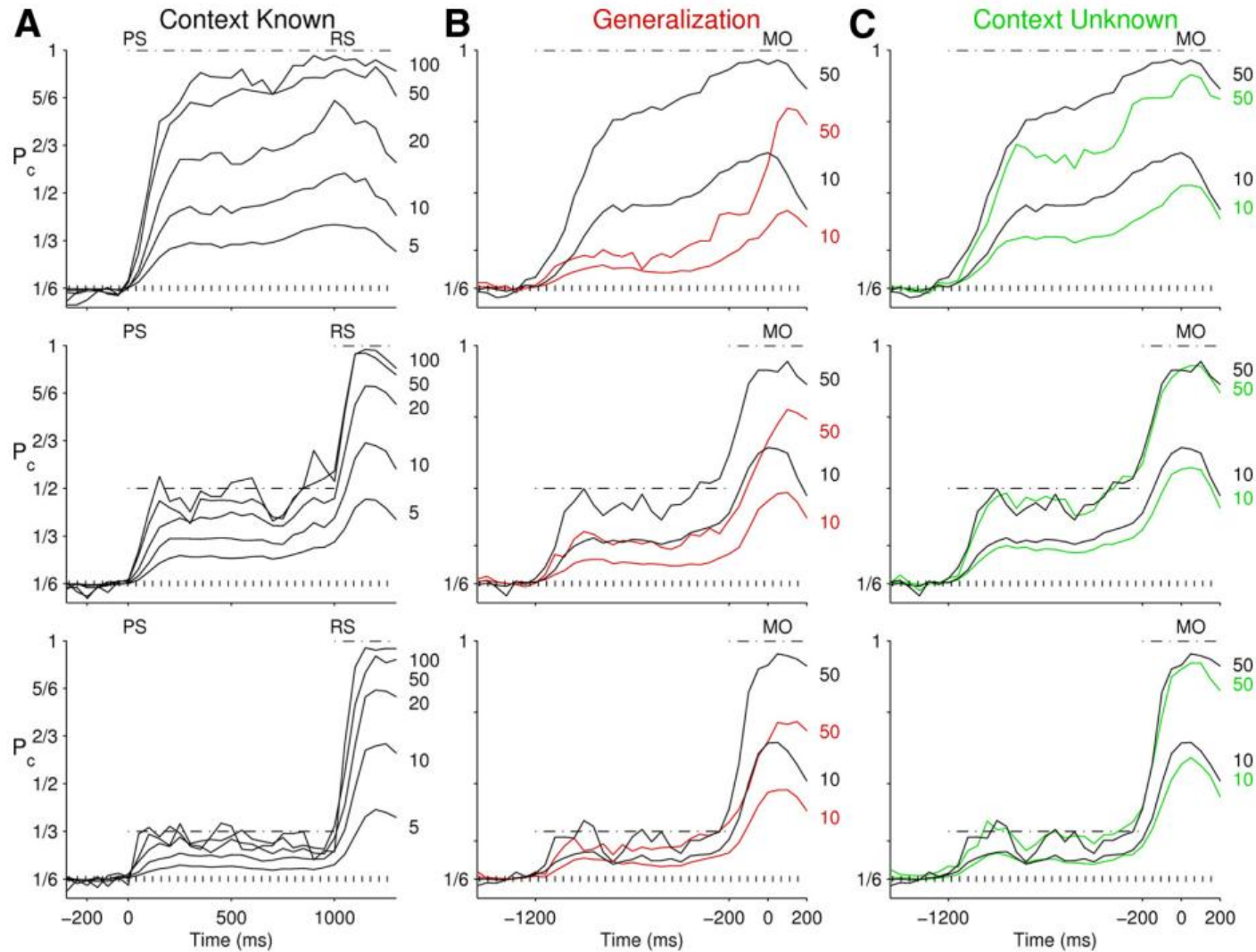
Rickert, Riehle, Aertsen, Rotter, Nawrot (2009) *J Neuroscience* 29

Time-resolved decoding from a neuronal population



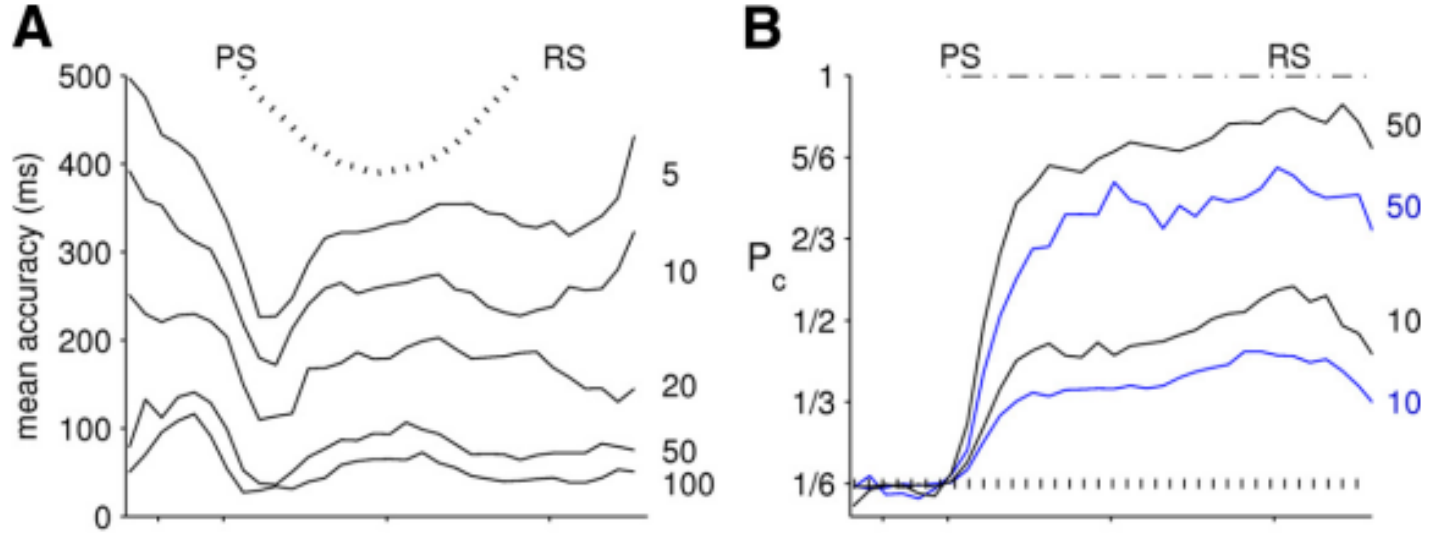
Rickert, Riehle, Aertsen, Rotter, Nawrot (2009) *J Neuroscience* 29

Time-resolved decoding from a neuronal population

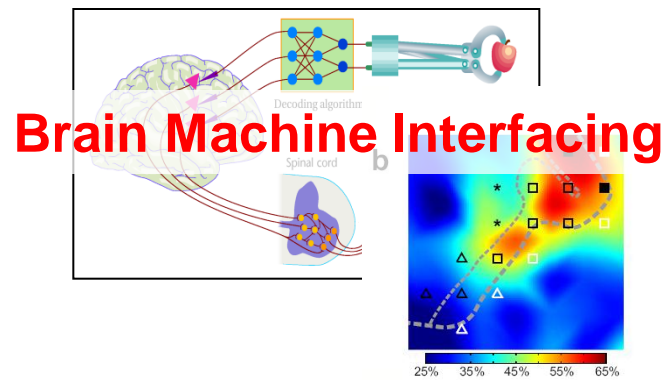


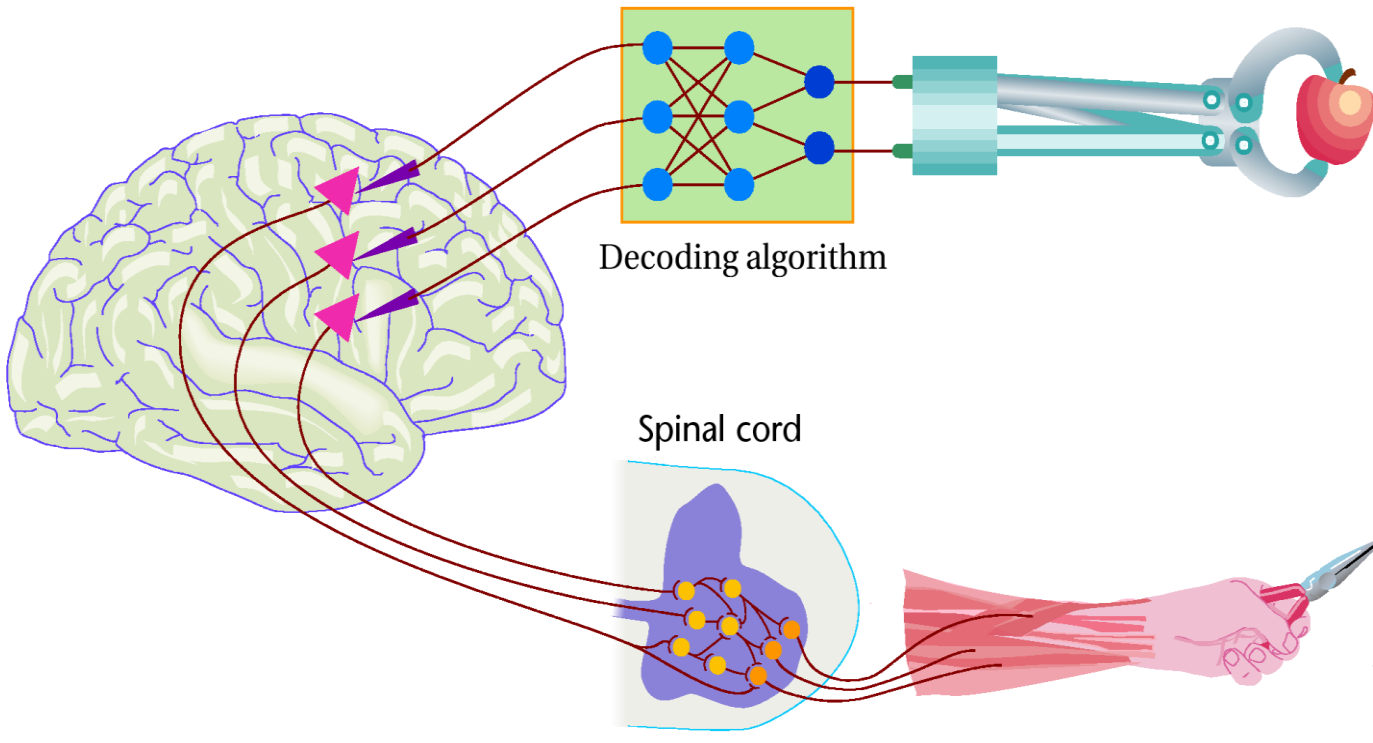
Rickert, Riehle, Aertsen, Rotter, Nawrot (2009) *J Neuroscience* 29

Decoding of Time and Direction

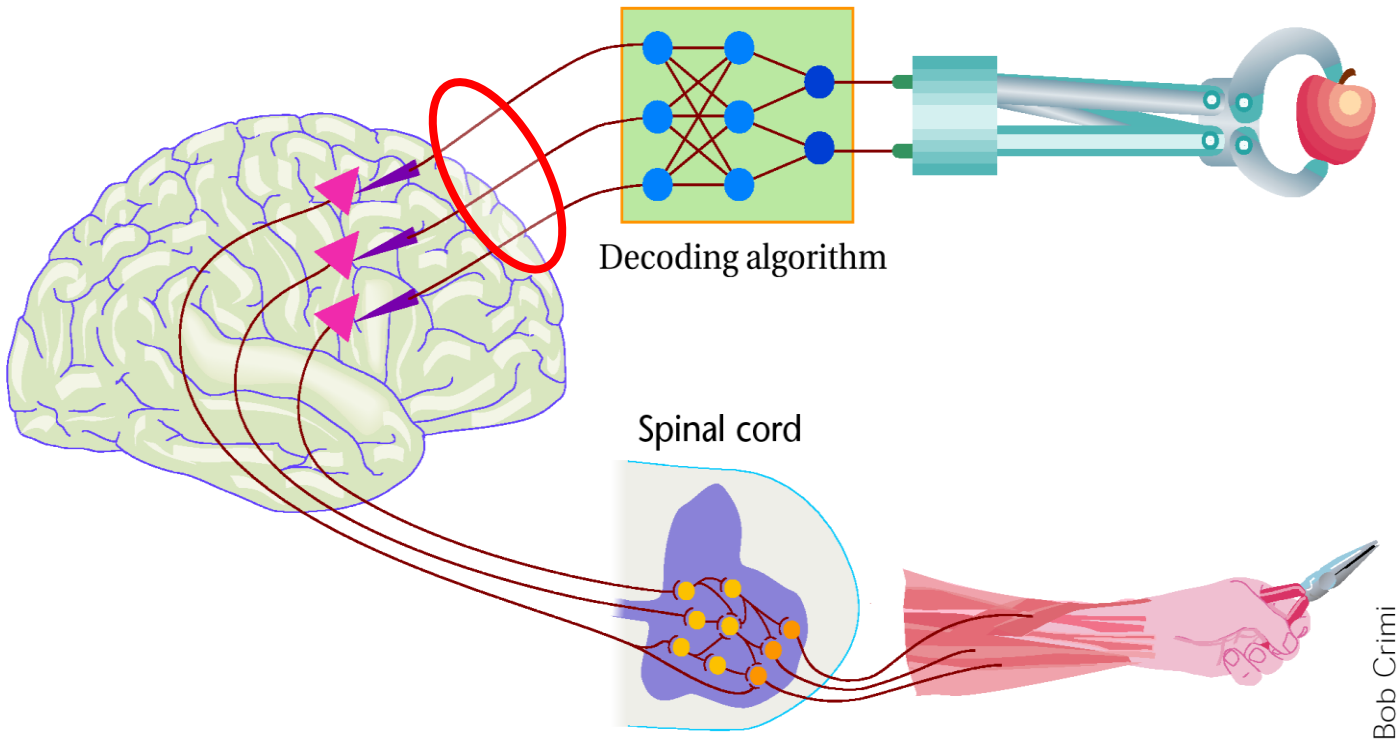


Brain – Machine – Interfacing (BMI)

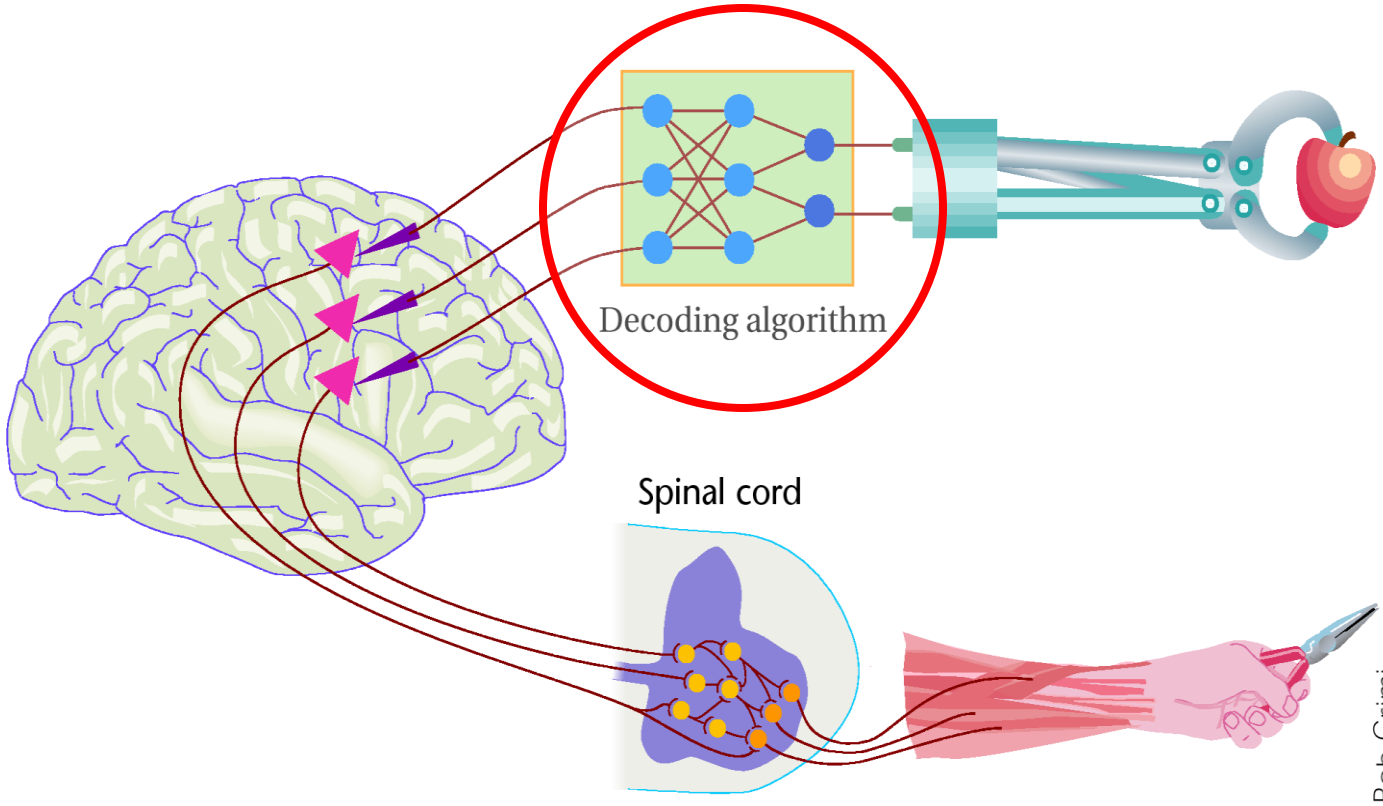




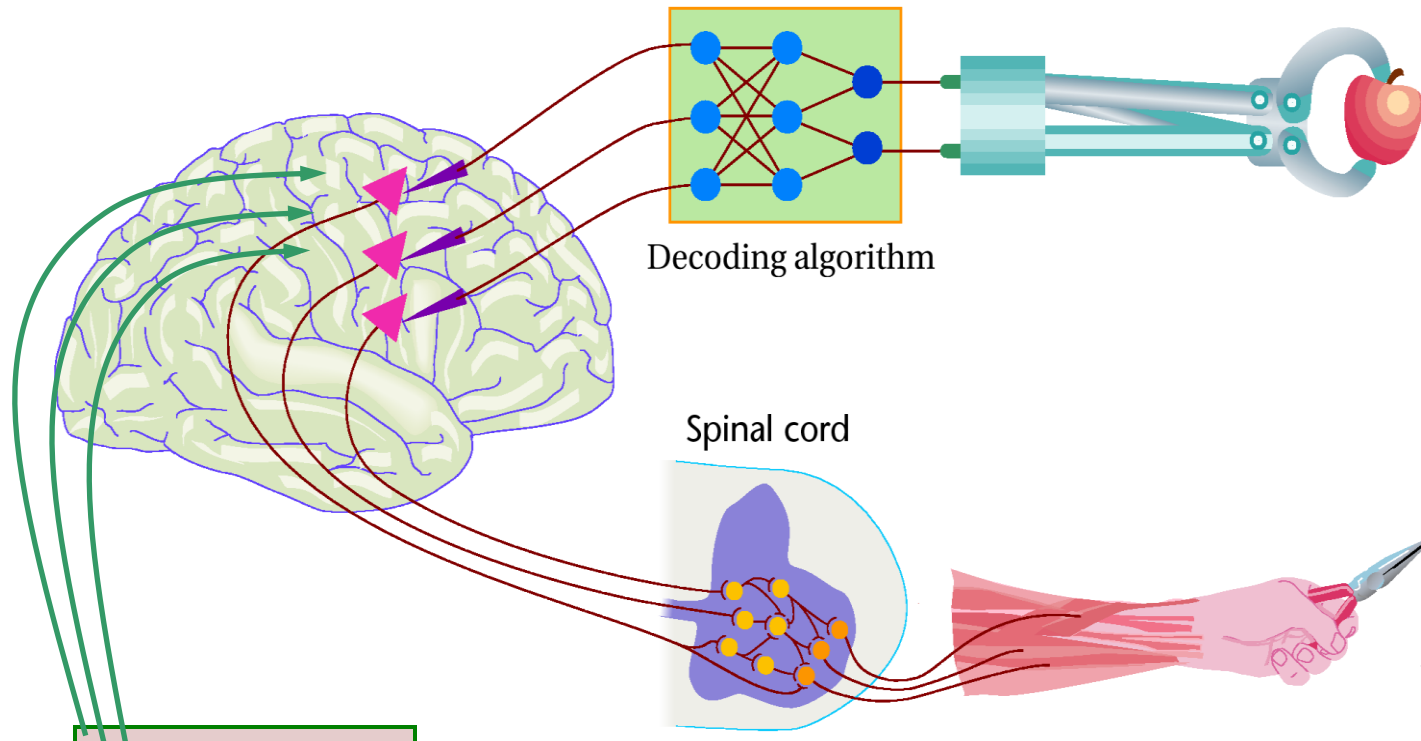
Fetz (1999) Nature Neuroscience



1. neural interface to non-redundant sources
2. spatio - temporal scale of brain signals
3. techniques for information read out
4. sensory feedback integration



1. neural interface to non-redundant sources
2. spatio - temporal scale of brain signals
3. techniques for information read out
4. sensory feedback integration



1. neural interface to non-redundant sources
2. spatio - temporal scale of brain signals
3. techniques for information read out
4. sensory feedback integration

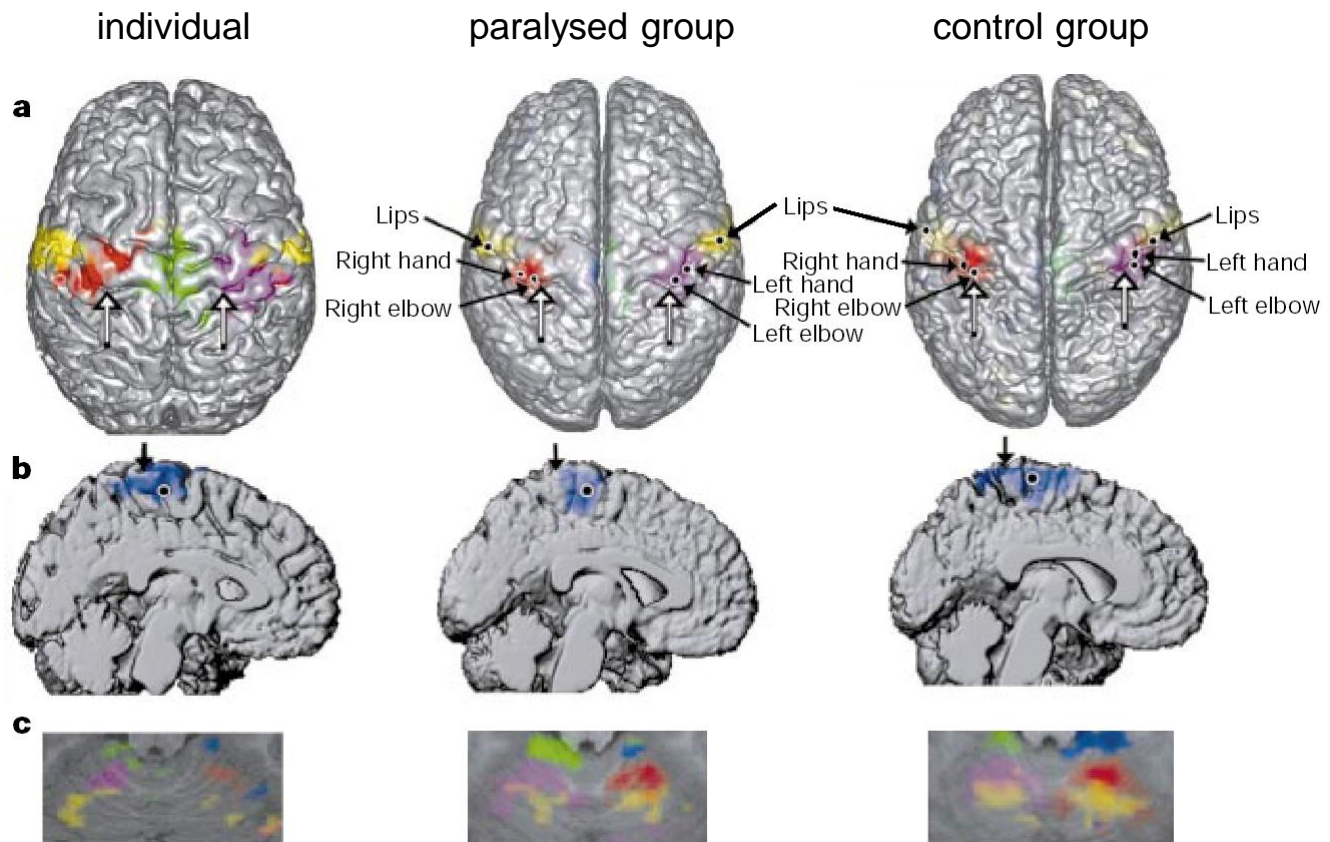


Figure 1 Cortical and cerebellar activation associated with attempted and executed movements in a paralysed individual (left), paralysed group (middle) and control group (right). **a, b**, Scaled integrals of t -test statistics (1.2 cm beneath the cortical surface); black dots indicate the location of t -value maxima. In **a** (top view), blue areas of activation are omitted from the left-side panel to avoid overlap; hollow arrows, putative hand-notches on the precentral gyri; **b**, mid-sagittal renderings of left-hemisphere activation resulting from attempted flexion of right toes. Arrows, central sulcus. **c**, Activation maps (SPM $\{t\}$) in axial sections through the anterior cerebellum (21 mm inferior to the anterior-posterior commissural line). Red, abduction-adduction of fingers on the right hand, and purple, left hand; blue, flexion of right toes, and green, left toes; yellow, lip pursing.

Shoham (2001) Nature 413

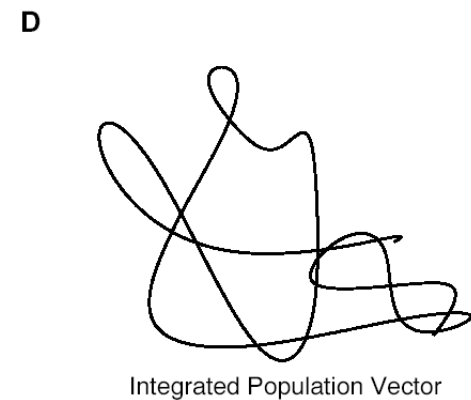
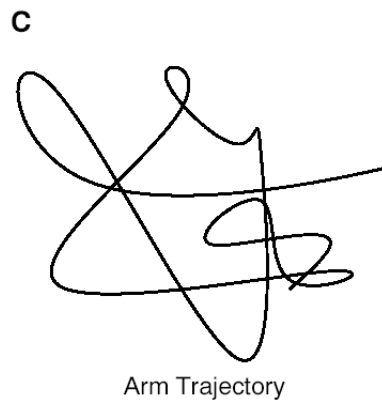
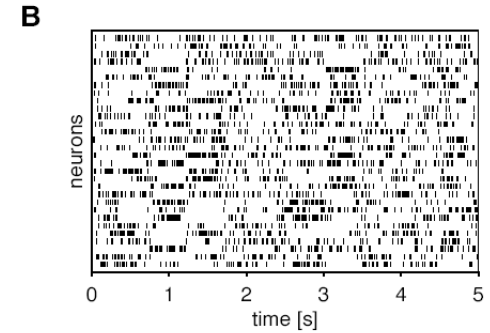
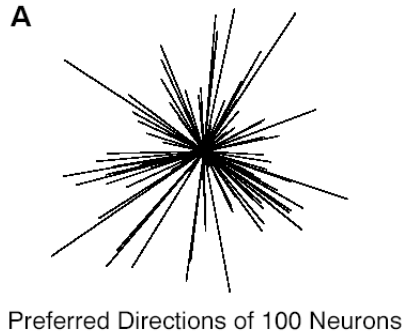
Decoding of instantaneous movement trajectory

Directional tuning:

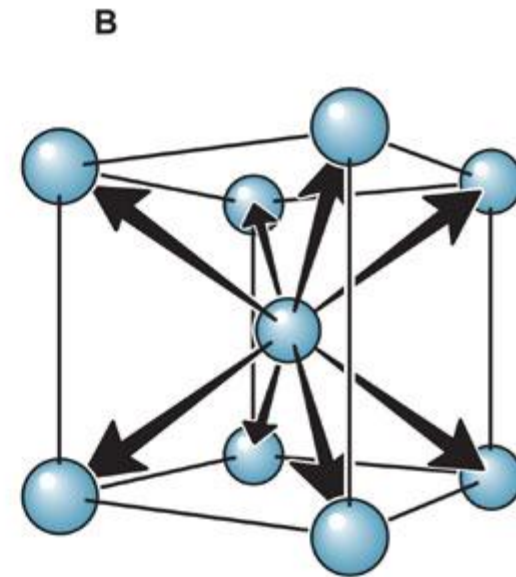
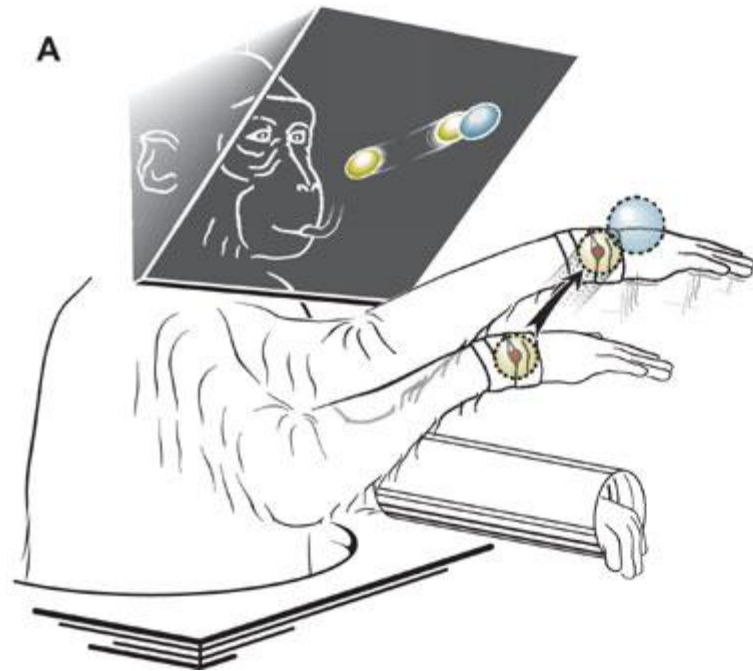
$$f_i(t) = g_i + \vec{p}_i \cdot \vec{v}(t)$$

Population vector:

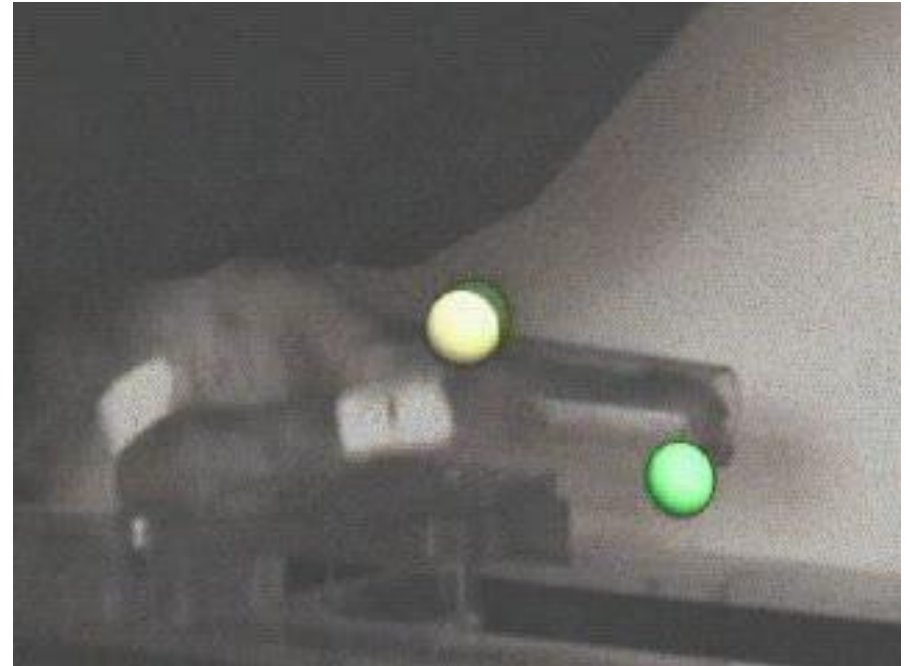
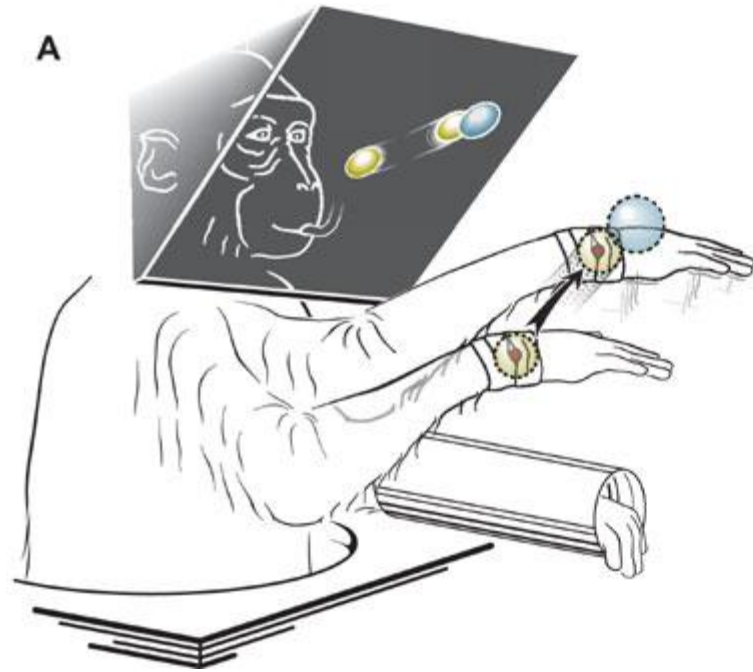
$$\vec{v}(t) = \sum_i [f_i(t) - g_i] \vec{p}_i$$



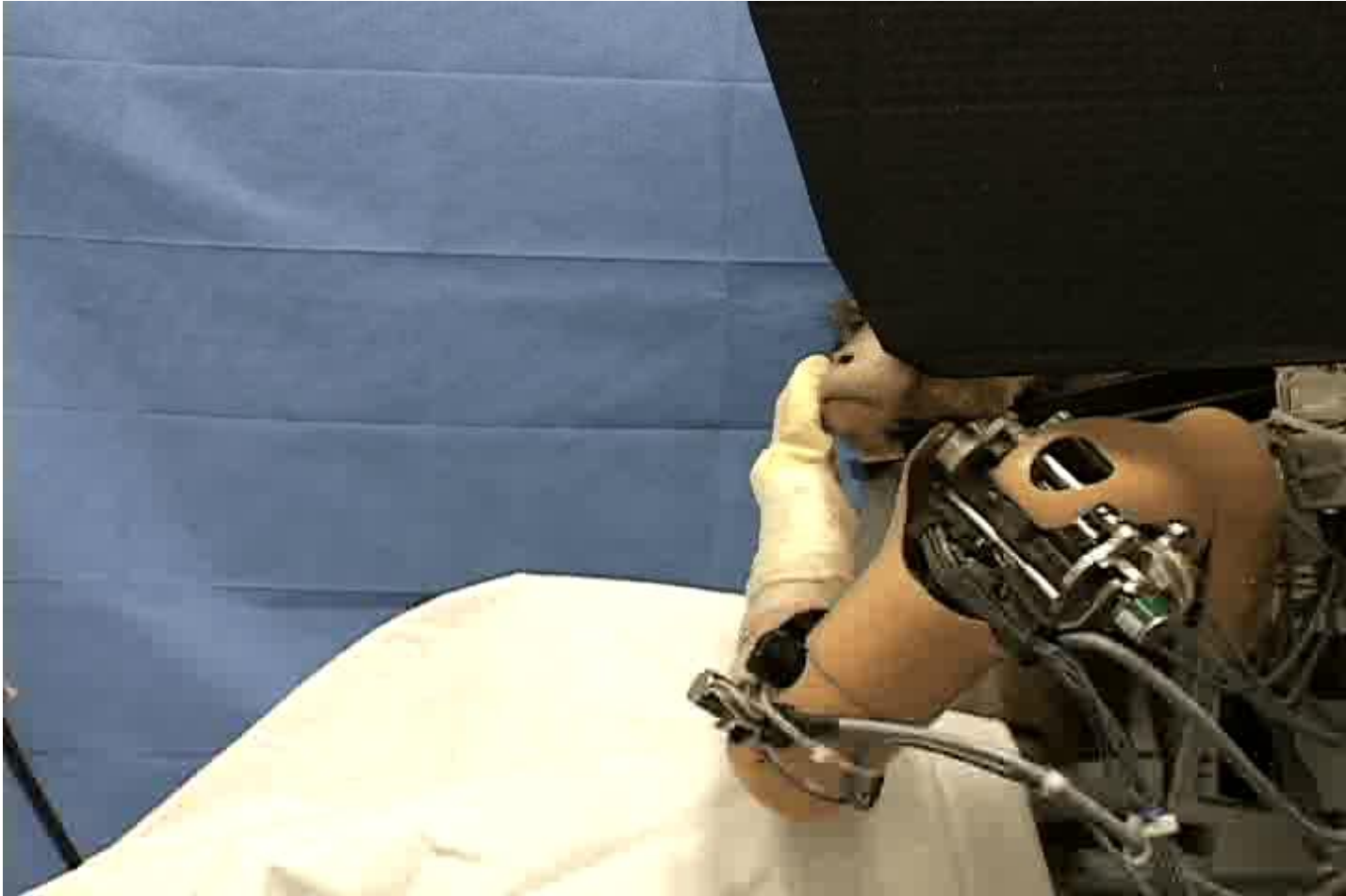
Nawrot, Aertsen, Rotter (1999) J. Neurosci. Meth 94.



Schwartz, Moran, Reina (2004) *Science*

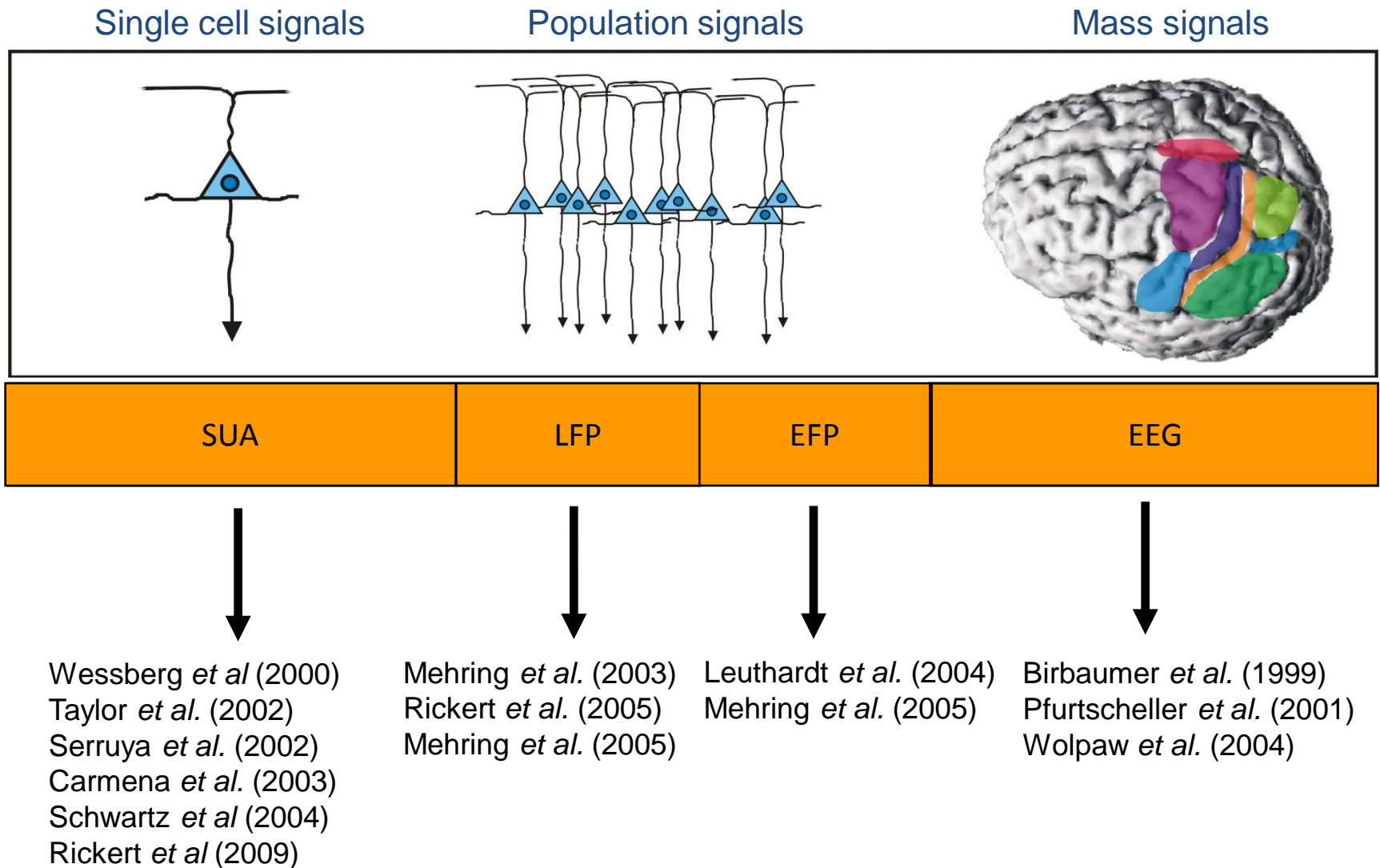


Schwartz, Moran, Reina (2004) *Science*



Decoding Population and Mass Signals

Brain Signals at Different Scales



Movement Information in Local Field Potentials (LFP)

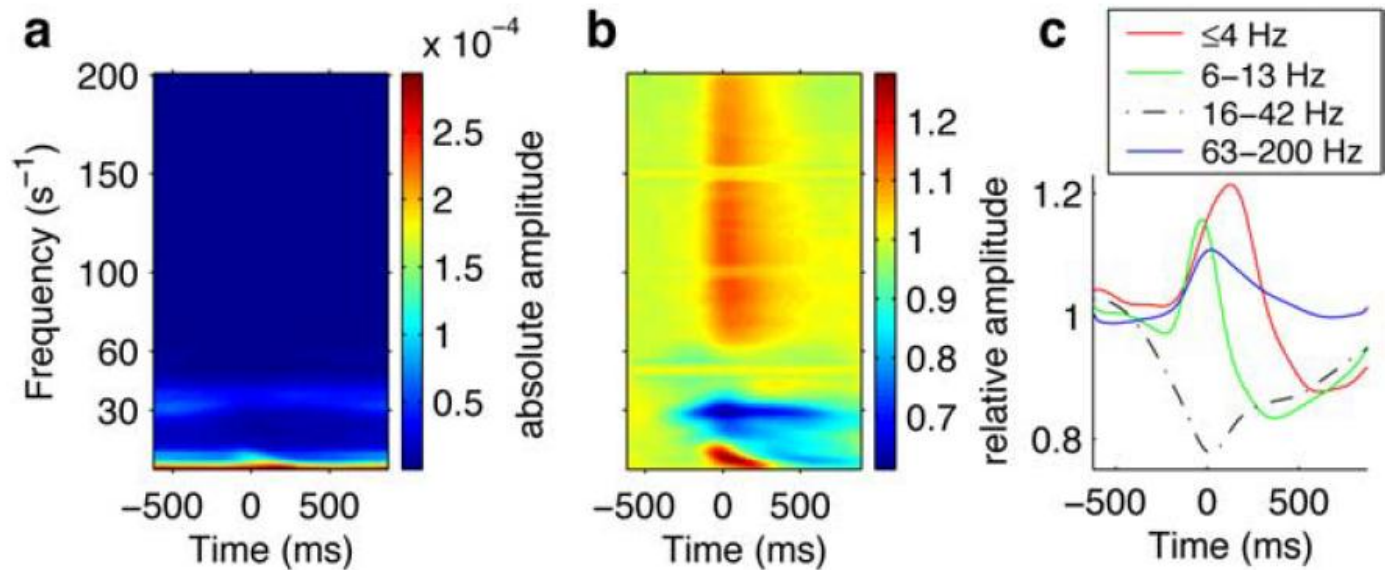
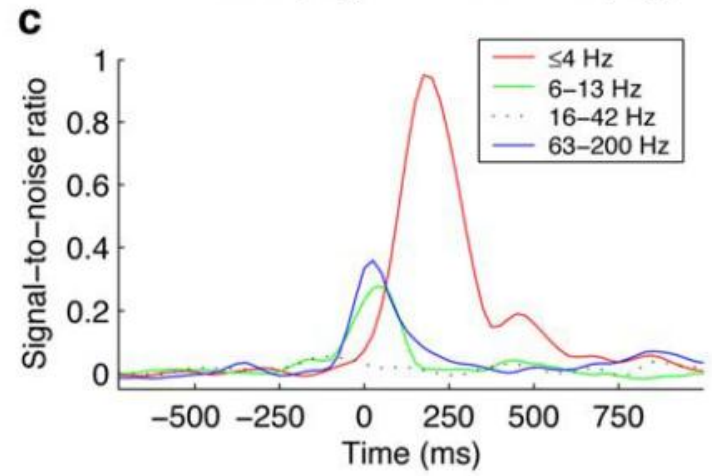
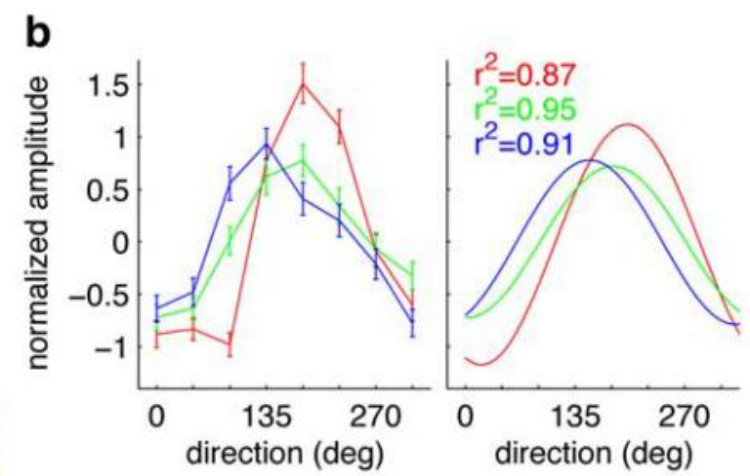
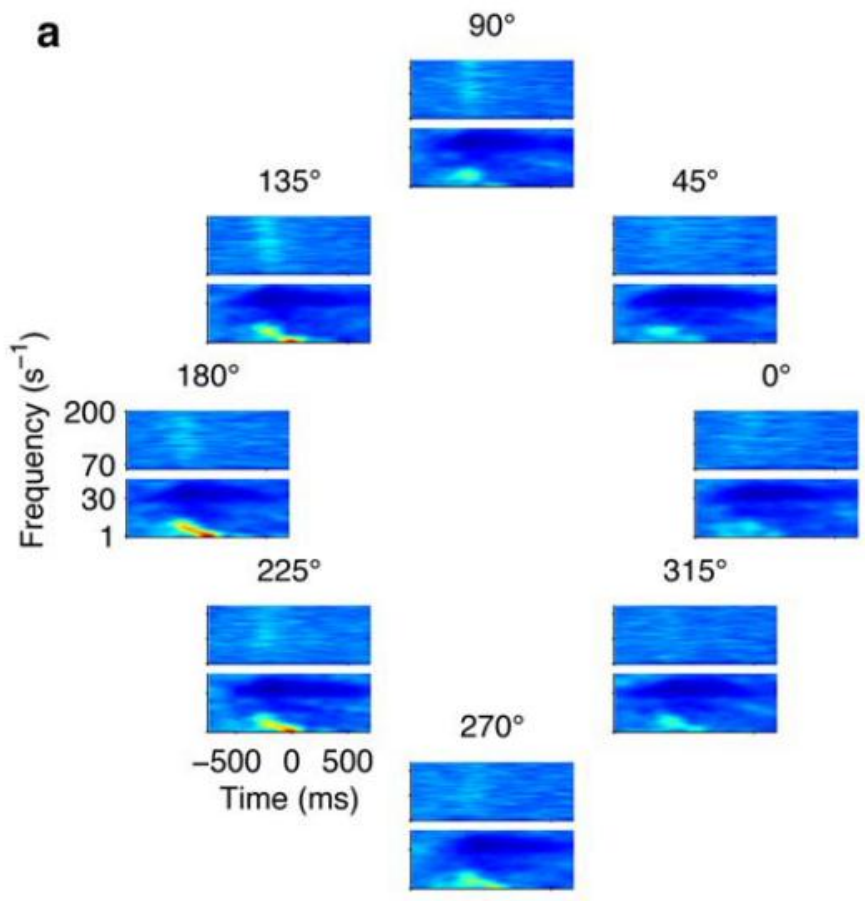


Figure 4. Characteristics of the LFP amplitude spectrum. Plots show averages across all electrodes and trials. **a**, Time-resolved amplitude spectrum (arbitrary units). The 50 Hz noise was removed by applying a notch filter centered at 50 Hz. **b**, Time-resolved amplitude spectrum as in **a**, each frequency bin normalized by its baseline amplitude (see Materials and Methods). **c**, Changes in amplitude exhibited by four different frequency bands (≤ 4 , 6–13, 16–42, and 63–200 Hz) during the task.

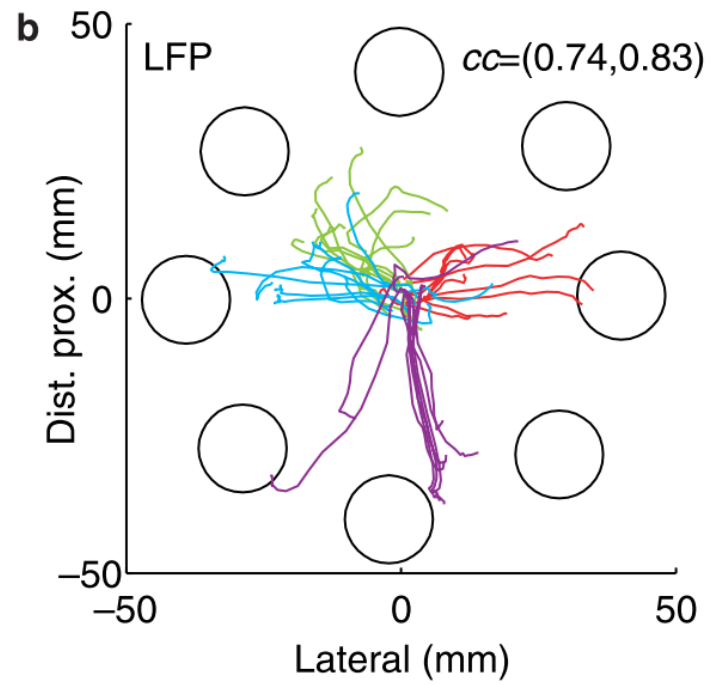
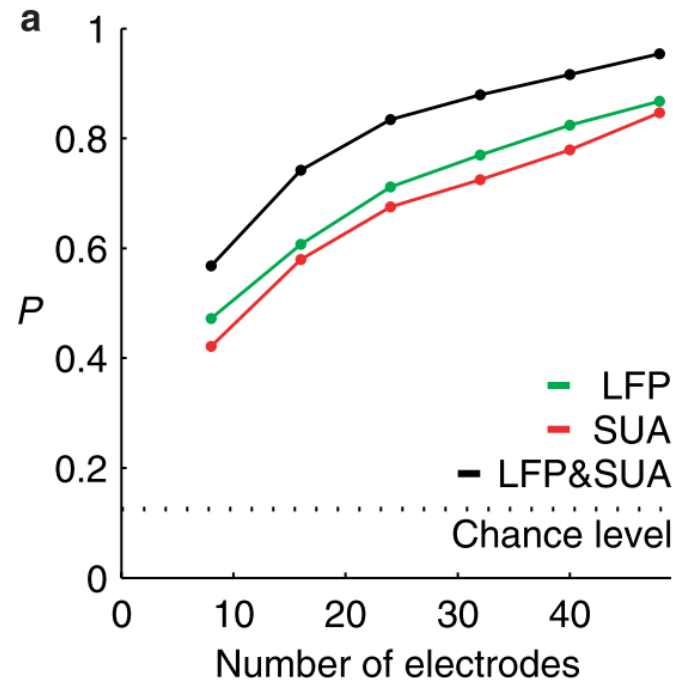
Rickert et al. (2005) J Neuroscience 25

Movement Information in Local Field Potentials (LFP)



Rickert et al. (2005) *J Neuroscience* 25

Movement Information in Local Field Potentials (LFP)



Mehring et al. (2003) Nat Neurosci 6

Movement Information in **Epicortical Field Potentials (EFP)**

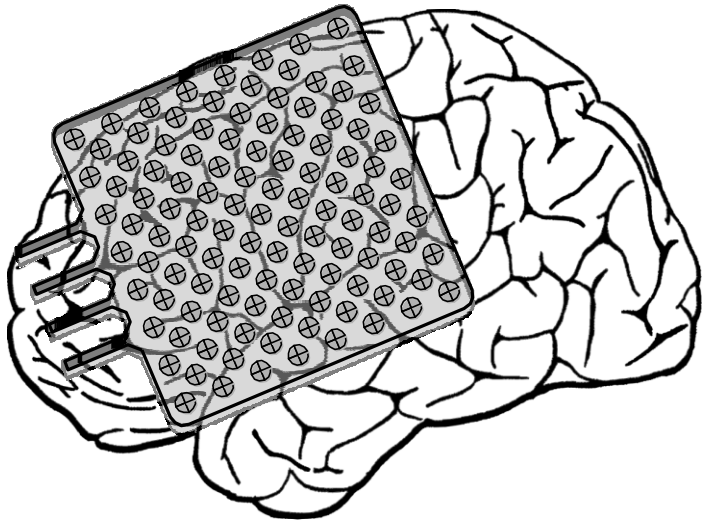
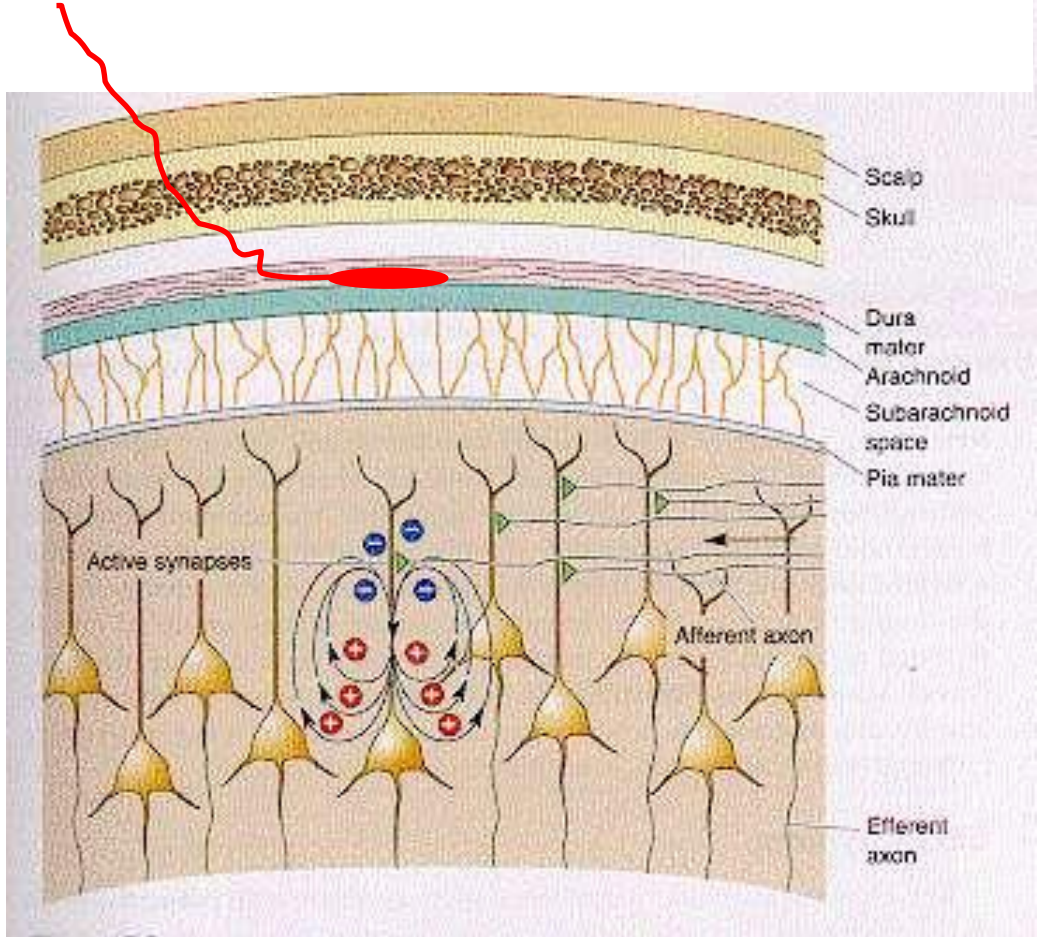
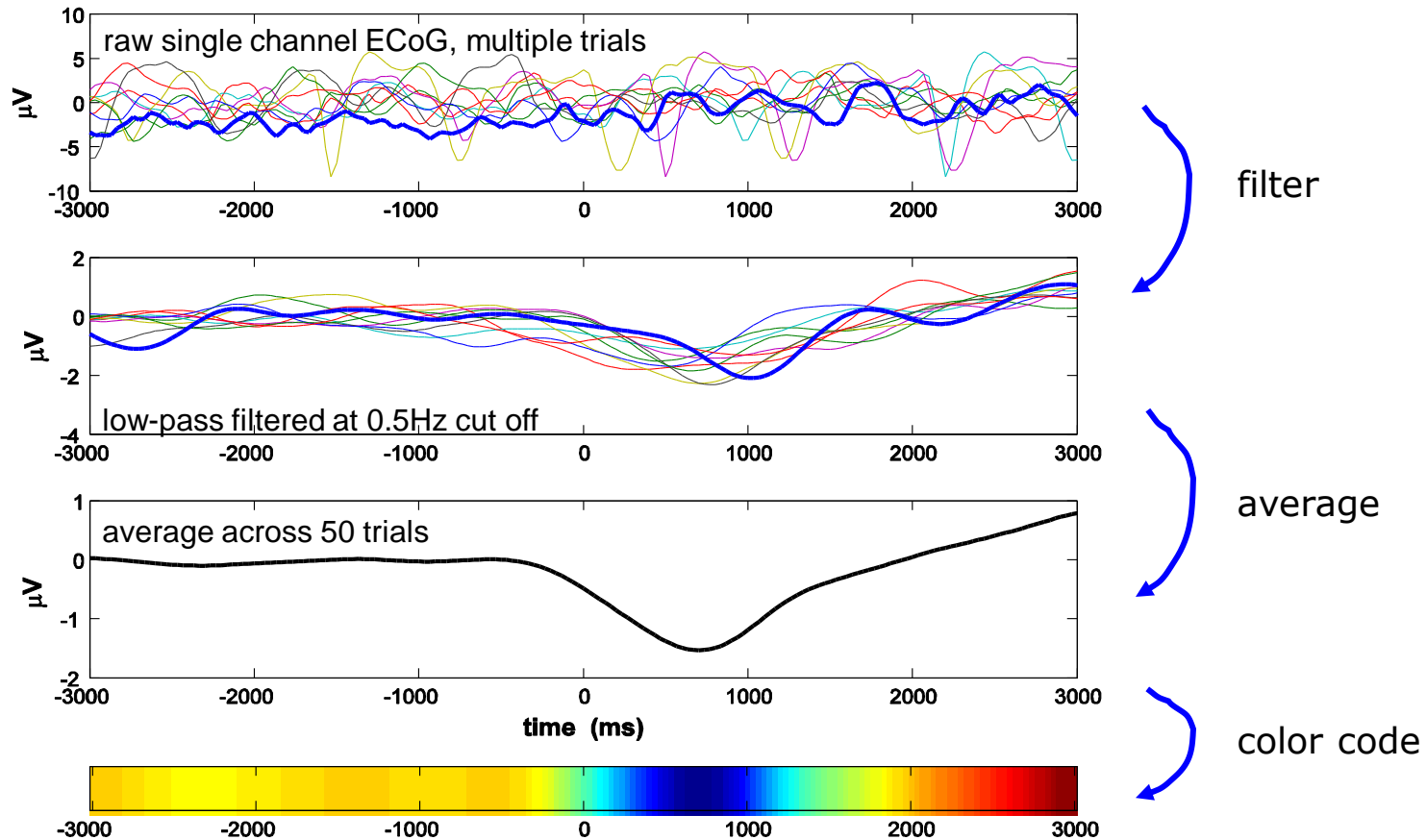


Photo: J Honegger, University Hospital Freiburg



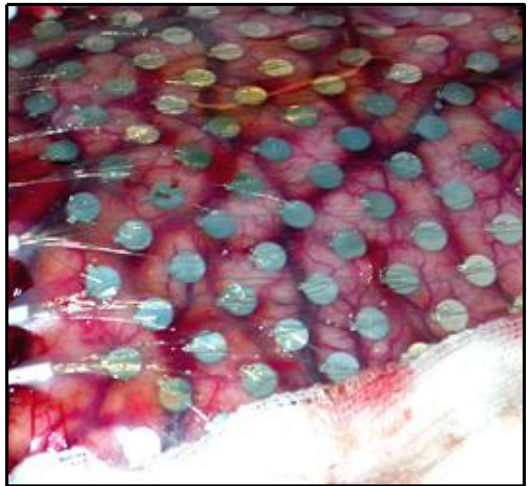
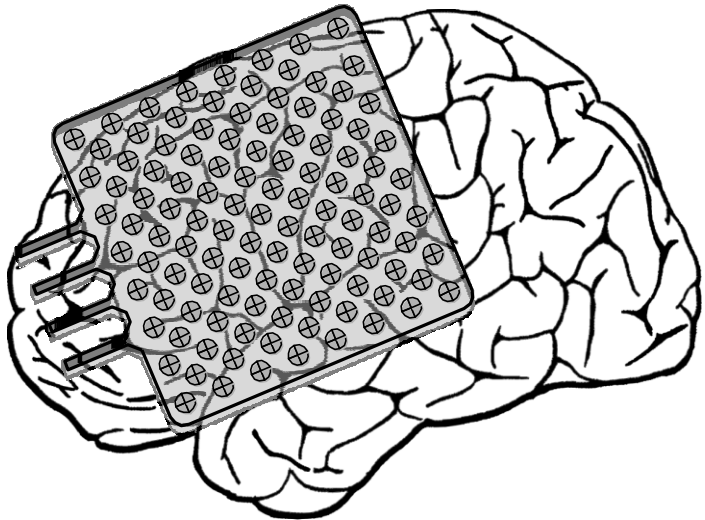
Mehring et al. (2004) J Physiol Paris 98

Movement Information in **E**picortical **F**ield **P**otentials (EFP)

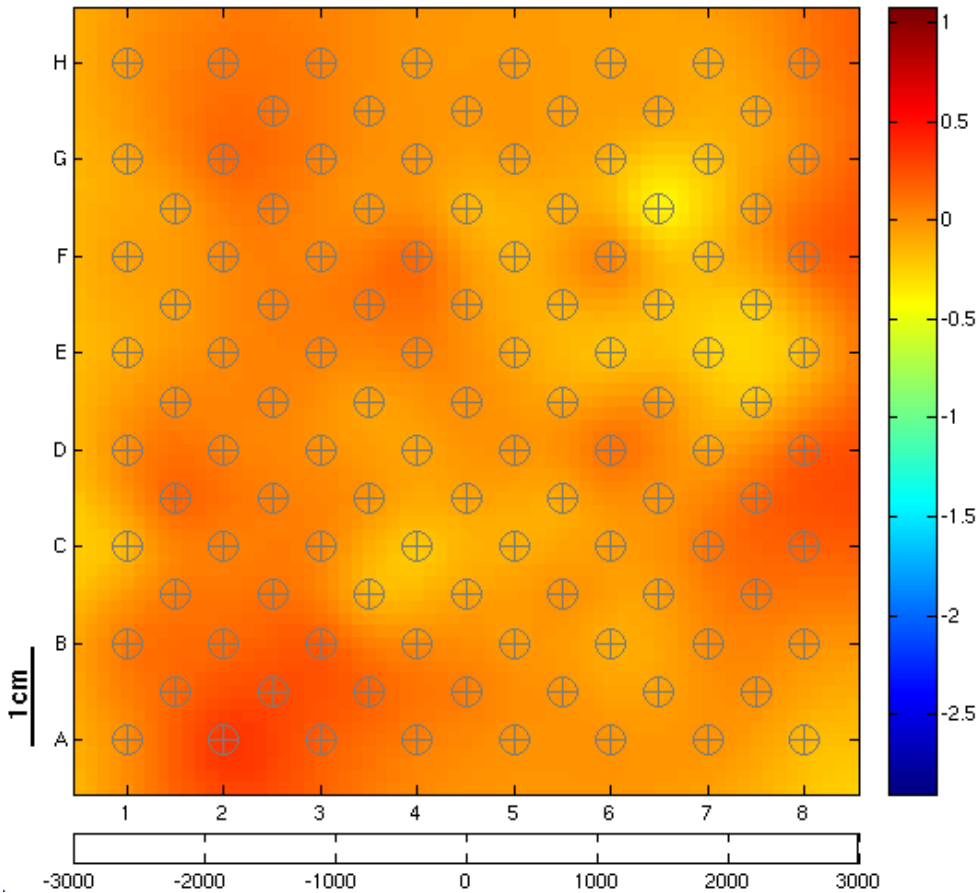


Mehring et al. (2004) J Physiol Paris

Movement Information in **E**picortical **F**ield **P**otentials (EFP)



Movement Related Potential



Mehring et al. (2004) *J Physiol Paris* 98

Movement Information in Epicortical Field Potentials (EFP)

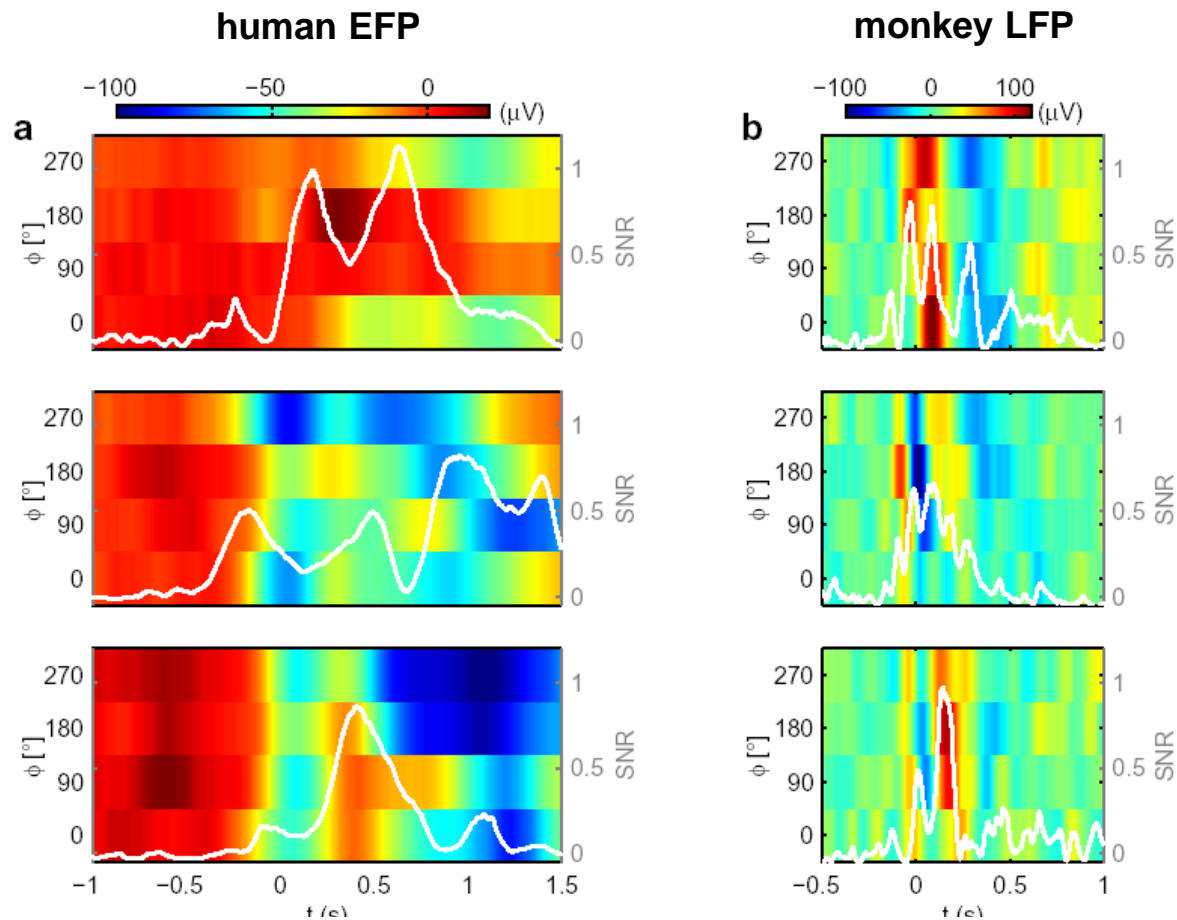
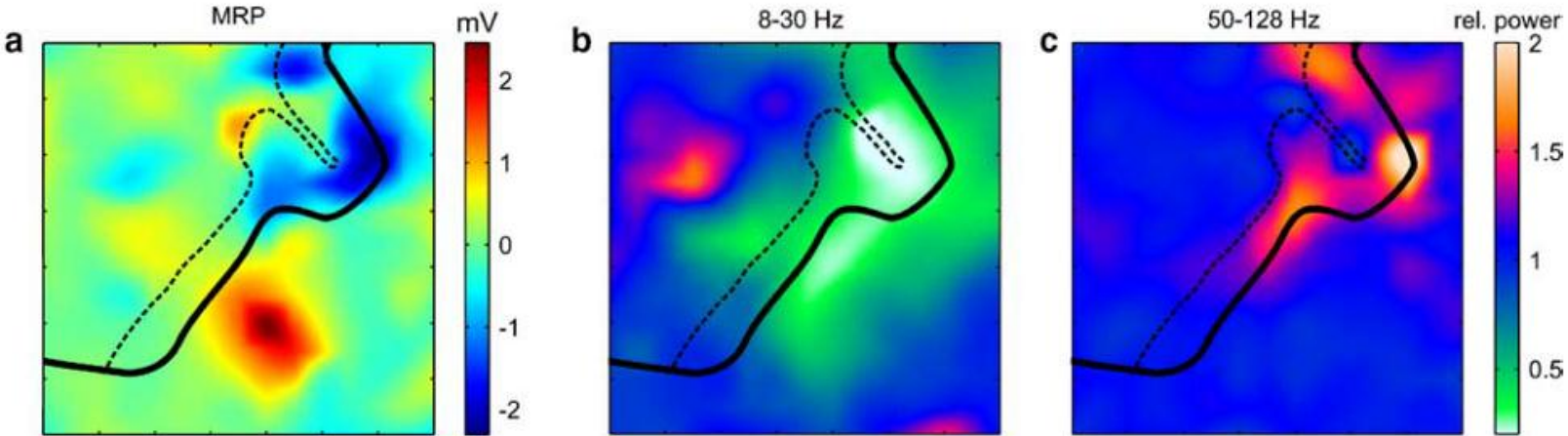


Fig. 5. Directional modulation of movement related potentials (MRPs) in single channel human EFP (a) and monkey LFP (b). The dashed lines denote the time of movement onset and the times of movement end. All examples were recorded from the hand/arm area of the motor cortex of the precentral gyrus. Trial-averaged potentials were calculated separately for the four movement directions from 1 s before to 1.5 s after movement onset (a), resp. from 0.5 s before to 1 s after movement onset (b). Direction of movement ϕ in degrees is assigned to the left ordinate, $\phi = 0^\circ$ corresponds to rightward movement; ϕ increases counter-clockwise, i.e., 90° corresponds to forward movement. White curves show the time course of the signal-to-noise ratio (SNR, see Methods). EFP examples represent channels with high SNR from all three subjects (S1, S2, S3 from top to bottom). LFP examples represent channels with peak SNR from the upper third of the peak SNR distribution. For a comparison of the complete distributions of the peak SNR of EFPs and LFPs see Fig. 6.

Mehring et al (2004) *J. Physiol Paris*

Movement Information in **E**picortical **F**ield **P**otentials (EFP)



Movement Information in Epicortical Field Potentials (EFP)

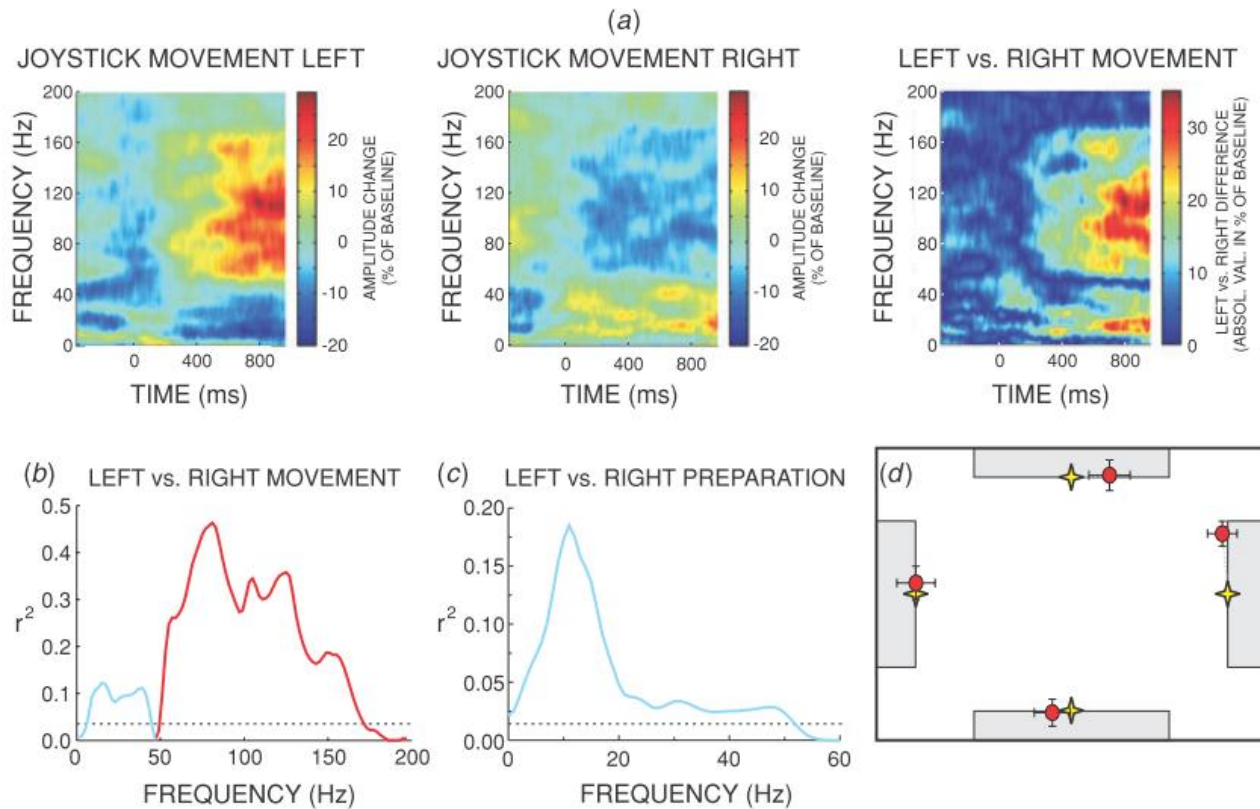
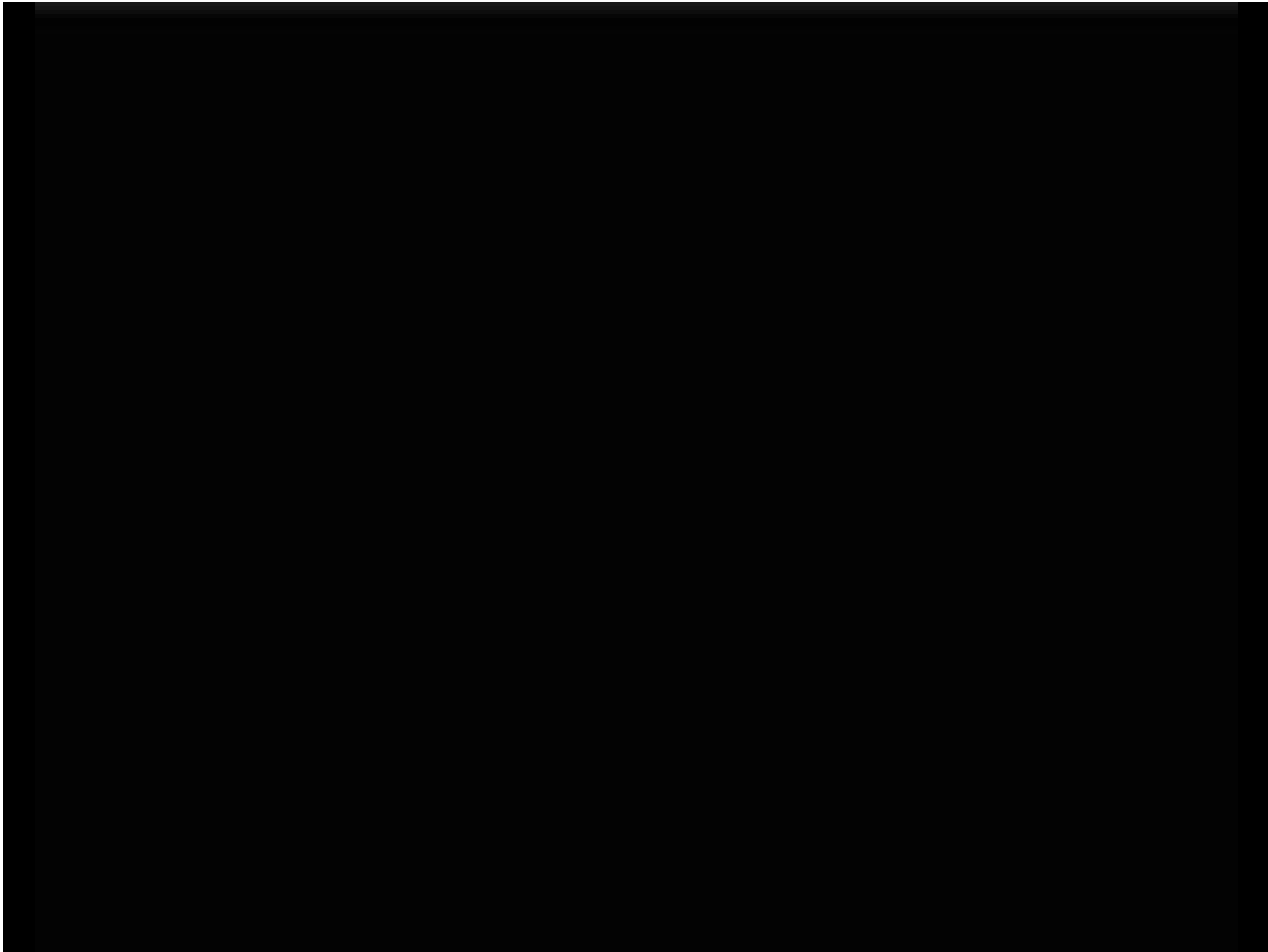


Figure 4. ECoG correlations with joystick movement direction before and during movement for patient D. At -400 ms the target appeared, and at 0 ms the cursor appeared and began to move controlled by the joystick. The patient's task was to move the cursor to a target at one of 4 or 8 locations (i.e., center-out task). (Figures (a)–(c) are based on the 8-location data set and are calculated for the left-most and right-most target; (d) is based on the 4-location data set.) (a) Left and center panels: time courses for left and right movements, respectively, of the amplitudes from 0–200 Hz of the difference between two adjacent electrodes. Right panel: the absolute value of the difference between left and right time courses. Movement direction is reflected in ECoG across a wide frequency range, including frequencies far above the EEG frequency range. In general, amplitudes at frequencies below and above 50 Hz change in opposite directions. (b) The correlation between the signal shown in (a) and movement direction over the period of movement execution. Correlation is much higher at higher frequencies not discernible in scalp EEG. (c) Correlation (for a single electrode location versus the remote reference electrode) with movement direction for the 400 ms prior to cursor movement. μ rhythm activity predicts movement direction. (In (b) and (c), — and — indicate negative correlation and positive correlation, respectively, with the amplitude of left movement minus right movement; and dashed lines indicate the value of r^2 that is significant at the 0.01 level.) (d) Average final cursor positions (●) predicted by a neural network from ECoG activity are close to the actual average final cursor positions (✦) (see text). (Error bars indicate the standard error of the mean.)



FIN